UiT
THE ARCTIC
UNIVERSITY
OF NORWAY

FACULTY OF SCIENCE AND TECHNOLOGY
DEPARTMENT OF PHYSICS AND TECHNOLOGY

Power Potential of Rystraumen, Norway

—

Kine Solbakken

EOM – 3901 Master's Thesis in Energy, Climate and Environment
March 2014

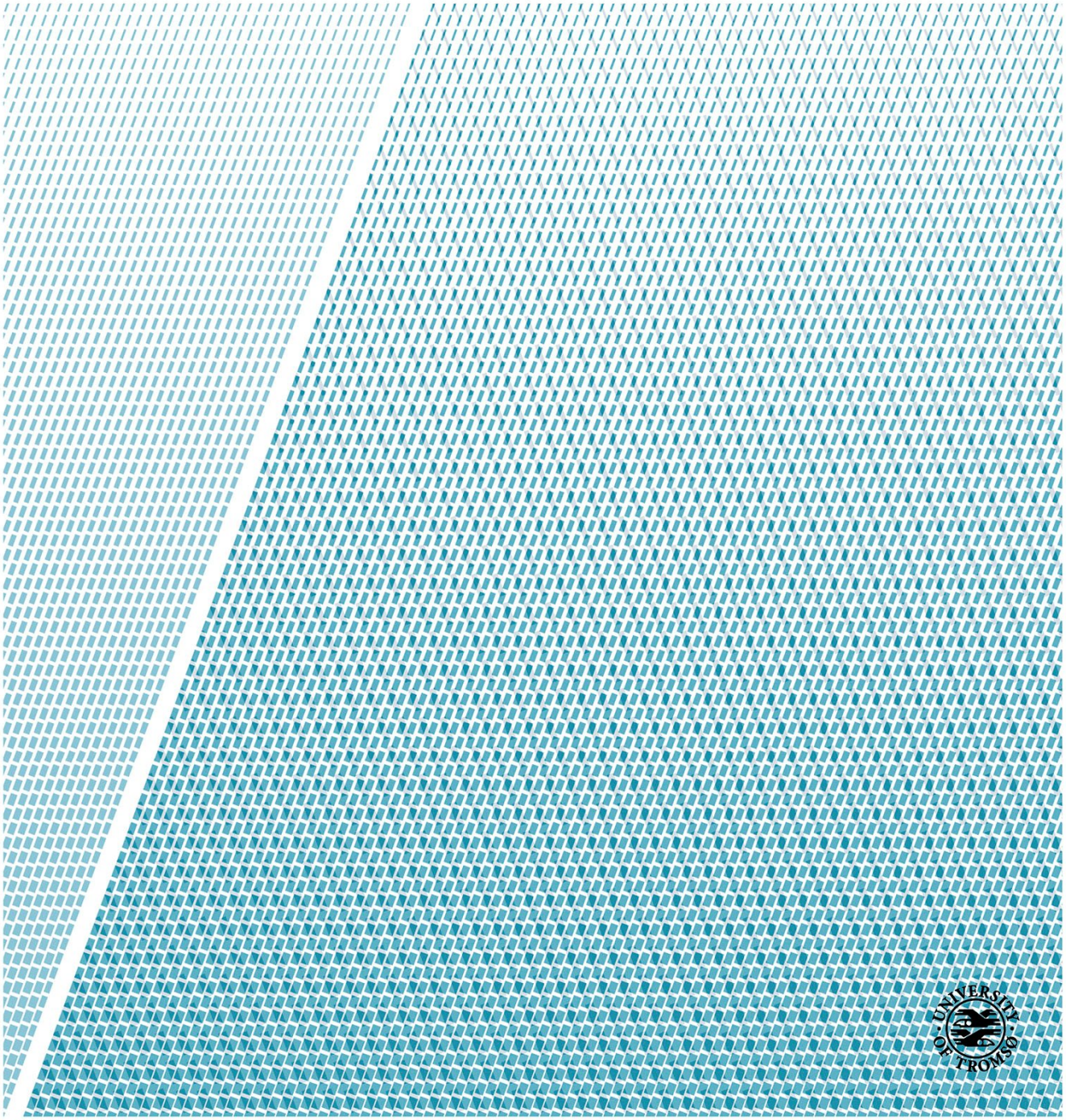

Abstract

The maximum power potential of the tidal current Rystraumen close to Tromsø, Norway, is assessed both theoretically and from a depth-integrated numerical model (FVCOM). For the theoretical estimate of the maximum power potential, the topography is simplified to the situation in which the channel connects a large basin, unaffected by the energy extraction, to a closed bay. A set of governing equations is simplified to one single equation, which balances the acceleration of the current velocity, the pressure gradient and the force associated with turbine friction. The theoretical estimate is calculated to 66 MW. From the numerical simulations the maximum power potential is estimated to be 40 MW if one allows for a uniform energy dissipation over one entire cross section of the channel. The reason for the difference in the theoretical and the modeled estimates is that in reality the flow of water is not entering a closed bay, but a pool which is connected to the rest of the sea through three channels. The same difference between theoretical and modeled results is reported in other studies where similar sitiuations have been considered.

Acknowledgements

I gjennom hele min studietid på Energi, Klima og Miljø har jeg aldri gått tidlig fra en eksamen, og siden masteroppgaven føles som verdens største eksamen sitter jeg her til siste minutt av de 161 280 minuttene jeg har hatt til rådighet på denne oppgaven.

Takk til Yngve som introduserte meg for temaet, fokuset har endret seg mye i løpet av prosessen men har endt opp like interessant som vi tenkte. Takk til min hovedveileder Ole Anders på Akvaplan-niva for uvurdelig hjelp og oppfølging, for at du alltid har tatt deg tid og for at ogs du synes dette har vært en spennende oppgave.

Takk til alle på Norut-brakka for alle kaffepausene og godt selskap. Takk til Tarjei for alle wienerbrødene vi har delt og til Kampffi for å alltid hjelpe meg med problemer i matlab. Takk til Karina for ditt gode humør og smittende latter, og resten av gjengen i Mackbratta. Takk til Jens for at du kom i rett tid da jeg trengte litt moralsk støtte og for korrekturlesing til siste minutt.

Contents

Chapter 1

Introduction

In the recent years there has been a growing interest in new and more efficient energy production from renewable resources. A major unused potential is the tidal current created as the water level rises and falls. When large bulks of water are transported and flow through narrow straits or around headlands, strong currents might occur. The kinetic energy can be exploited using simple turbines, much similar to wind-turbines. The tidal turbines are considered to be very environmental friendly. They are often fully submerged and therefore have no visible impact on the surroundings.

How to theoretically estimate the power potential of a tidal current has been investigated in several recent studies. In this study the power potential of Rystraumen close to Tromsø will be investigated. Until now, there exists no simple formula to estimate the maximum power potential of a tidal current applicable for any situation [Garrett and Cummins, 2005]. For one single turbine in a flow the maximum power dissipated by the turbine is calculated from the kinetic energy flux through the area spanned by the turbine. But when several turbines are combined into a farm of turbines, the situation becomes more complex. It has been reported in several studies that there is no easy relationship between the available energy for extraction and the kinetic energy flux of the undisturbed flow [Garrett and Cummins, 2004, Garrett and Cummins, 2005, Sutherland et al., 2007].

An attempt has been made to estimate the power potential both in Europe and in Norway. Despite of uncertainties, the conclusion is that tidal current is a major unused resource [European Commission, 1996],[Enova SF, 2007, Grabbe et al., 2009]. In a report from the European Commission *"Non-*

nuclear energy - JOULE 2" from 1996 it is estimated that energy from tidal currents and other marine currents possibly has a potential of supplying Europe with 48 TWh per year [European Commission, 1996]. An assessment of the energy potential in the currents along the Norwegian coast was done by a private consultant for the public enterprise owned by the Norwegian Ministry of Petroleum and Energy, Enova SF in 2007. The realistic potential of energy extraction from tidal currents in Norway was estimated to be less than 1 TWh/year [Enova SF, 2007].

Even though the reports from both Enova and the European Commission agree that the energy created by the tide is an unused resource with a large potential, there are uncertainties related to the estimations of the power potential. The uncertainties are related both to how the power potential has been calculated and to the data on which the estimations are based.

New technology for energy extraction is developing fast. At present time, only single turbine projects are converting the kinetic energy from tidal currents into electricity. However, it is assumed that within a decade, full scale turbine farms will be operating, and more energy will be extracted from each channel [Enova SF, 2007]. In the reports from Enova and the European Commission the estimations of the power potential are both based on the energy flux as it has been common to assume that the energy available for extraction is some percentage of the energy flux of the undisturbed flow [Garrett and Cummins, 2005], [Sutherland et al., 2007]. To meet the need for a simple and cost efficient way to estimate the power potential of currents several studies have developed formulas for power potential estimation [Garrett and Cummins, 2004], [Garrett and Cummins, 2005]. However, these studies are limited to simplified situations. The current in Rystraumen does not satisfy the assumptions made in these studies.

Rystraumen is located in Northern Norway, close to the city Tromsø. The current velocity is expected to exceed $3m/s$ [Grabbe et al., 2009]. During 2014 the Norwegian company Flumill will test a pilot project, also called Flumill, in Rystraumen. The project has got a concession to test a turbine of 0.5 MW. If the testing of the turbine goes well, the next step is a small farm consisting of three turbines with a potential of extracting 5 MW in total.

The tidal current in Rystraumen is created as the tidal wave is funneled between the mainland and the islands Senja and Kvaløya. The topography forms a complex system which makes it difficult to theoretically estimate the power potential of the current. Energy extraction introduces a resis-

tance to the flow and the water might be diverted away from the channel if the resistance is significant. Also, locally in Rystraumen, the channel splits into two sub-channels, which makes the situation even more complex. As more resistance is added to the larger sub-channel where the turbines will be introduced, more water might be diverted into the smaller sub-channel.

The equations presented in Garrett & Cummins (2004) and Garrett & Cummins (2005) will be further developed to better suit the situation of Rystraumen. The new equation will be used to estimate the power potential of Rystraumen and will also be compared to estimates obtained from the formulas given in Garrett & Cummins (2004) and Garrett & Cummins (2005). The estimates will be discussed and compared to the power potential calculated from velocity data obtained from numerical simulations of the flow. To simulate the tide in Rystraumen a depth-integrated Finite-Volume Coastal Ocean circulation Model (FVCOM) is used. The model is presented in Section 5.1.

In addition to the problem of deciding the power potential, there are issues related to the environmental impact when energy is removed from a current which need to be investigated. It is assumed that the direct impact on the environment where the turbines are submerged will be small, since the turbines will not be in any conflict with marine species. But what is assumed to be the greatest impact is that one removes a certain amount of energy from the current, lowering the energy and the velocity in the current. Possibly the amplitude of the tidal wave locally is also reduced [Rourke et al., 2010]. The possible environmental impacts due to energy extraction in Rystraumen, important and interesting as they are, will not be discussed here.

1.1 Tide and tidal currents

The variation in tide is driven by the gravitation forces between the moon and the earth in combination with rotation of the earth. Theoretically this means that at each place on earth were water is present there will be a two-time daily rise and fall in the sea level [Elliot, 2004]. The gravitational pull from the moon draws the water towards the side of the earth facing the moon. This effect creates one large high tide on one side of the earth and one smaller high tide on the other side.

The centripetal effect also gives rise to the tide. This can be explained by

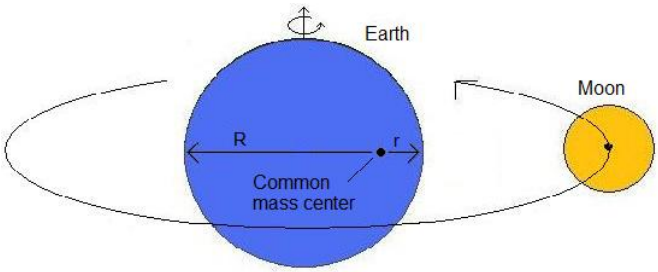

Figure 1.1: The moon orbits around the earth and gives rise to a two time daily rise and fall in sea level.The drawing is made with inspiration from Elliott (2004).

viewing the earth and the moon as one system with one common mass center which they spin around as in Figure 1.1. Their common mass center will lie just below the surface of the earth. The side of the earth facing away from the moon will have a radius from the mass center which is much larger than the radius of the side facing the moon. Therefore the velocity on the side facing away from the moon will be high and create a strong centrifugal effect. A mass in movement will always try to continue straight forward instead of following a circled path. This will make the water bunch up and create high tide. Also the side closest to the moon will experience the centrifugal effect. This will be much smaller, as the radius from the mass center is much smaller. These two high tides, due respectively to lunar gravitational pull and the centripetal effect, should theoretically be approximately the same size. This is called the semidiurnal lunar tidal constituent and is denoted M_2 [Pugh, 1987]. In practice, the size of the tides around the earth will differ significantly due to the tilt of the earth relative to the moon's orbit around the earth, the Coriolis effect, and especially because of different topographical effects [Elliot, 2004]. This gives rise to what is called overtides M_4, M_6 and M_{10}. These are especially important in estuaries and shallow water.

The sun also has an attractive force on the sea, and gives rise to a second semidiurnal tide denoted S_2 [Pugh, 1987]. When the moon and the sun are lined up with respect to the earth, the two semidiurnal tides, M_2 and S_2 sum up to create a large tidal range, called spring tide, as shown in Figure 1.2. When the moon and the sun are at right angles, the two forces pull in different direction and the two constituents M_2 and S_2 are out of phase, which creates a rather small tidal range, called neap tide [Carballo et al., 2009].

The tide, which gives rise to the surface elevation, is made up of several tidal constituents. The surface elevation is given by the following equation

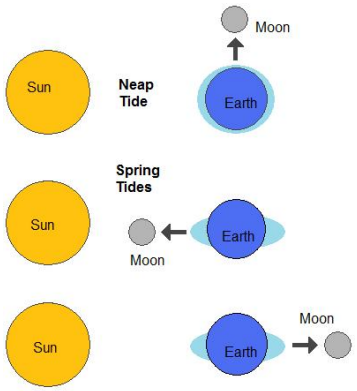

Figure 1.2: The sun gives rise to a second semidiurnal tide. The sun and the moon aligned gives rise to the spring tide. The drawing is made with inspiration from Elliot (2004).

$$\zeta = \sum_n a_n \cos\left(\omega_n t + \varphi_n\right) \tag{1.1}$$

t is time, n is the number of the tidal constituent. Each constituent is given as a cosine function with the amplitude a_n, the frequency ω_n and phase φ_n [Carballo et al., 2009, Defne et al., 2011].

In the Arctic seas the dominant tidal constituent is M_2 with a a frequency of 12.42 hours and an amplitude $a \approx 1m$ [Padman and Erofeeva, 2004]. In the report by Aquatera Ltd (2013) the mean spring tidal range is given as $2.1m$.

1.2 The Flumill pilot project

The company Flumill has developed a new and innovative technology for energy extraction from a tidal current. The technology has already been tested on a smaller scale and is now ready for the next step: full scale testing of the system in Rystraumen [Flumill, 2014]. The company has been awarded with prizes for innovative thinking. Among others, The Norwegian public enterprise Enova has granted the company significant financial support. Enova considers the project to be one of the most important projects for the development of tidal turbines, not only in Norway but also internationally [Enova, 2014].

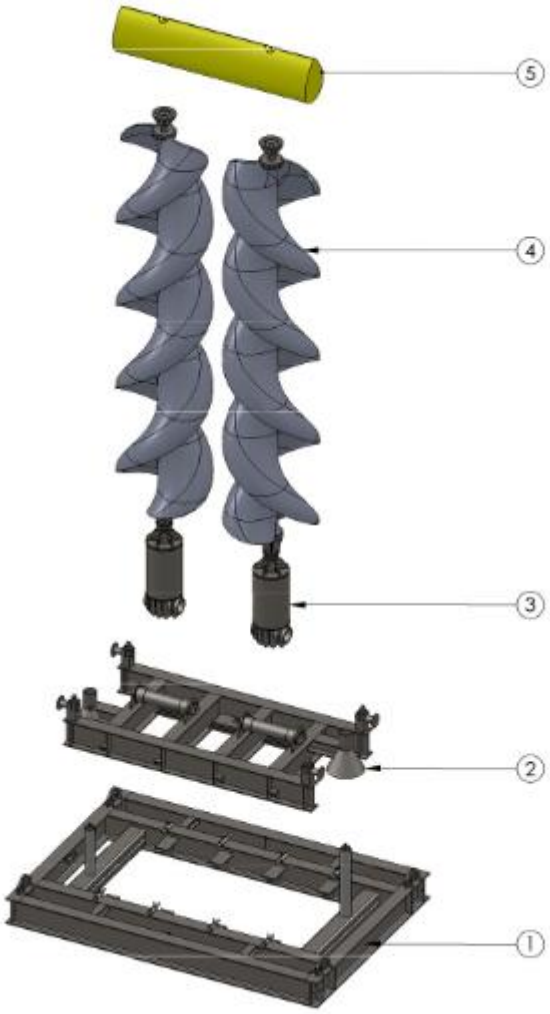

Figure 1.3: The Flumill 0.5 MW tidal turbine with a total height of 32m *[Flumill, 2014].*

The technology developed by Flumill is a turbine which also has the name Flumill. The device consists of four main parts: pivot, generators, turbines and a top fin as shown Figure 1.3. The 32 meter high installation will be mounted to the sea floor with a steel foundation. Two helix shaped vertical axis turbines will capture the kinetic energy in the current. These turbines will be counter rotating: one turbine will rotate clockwise while the other turbine counter clockwise. The outer part of the turbines will never exceed the current velocity, which contributes to low turbulence downstream of the device [Flumill, 2014]. As a result of this, turbines in an array might be placed closer to each other as the flow recovers faster. Another advantage of the low angular velocity is that it is rather harmless for marine species.

On the top of the turbines, a buoyant fin is mounted. The fin has two tasks: it supports the structure, and it makes it possible to change the operating angle. The latter makes it possible for the turbine to extract energy from the current on both ebb and flood. It also enables the turbines to adjust the operating angle to ensure maximum utilization of the energy in the flow. When the flow changes direction the buoyant top fin follows. Depending on the strength of the current, the helix turbines will obtain an operational angle of 25° to 50° [Flumill, 2011]. Another important feature of the Flumill device is that the area of the supporting structure is small and therefore the loss of energy in the current due to non-producing drag is low.

The technology has already been tested on a smaller scale, but is now ready for power generation in Rystraumen. The goal of this pilot project is to test the technology under real conditions and later commercialize the project both in Norway and internationally. The Flumill system can operate in tidal currents with a velocity as low as $1m/s$.

1.3 Structure of thesis

The report is structured in the following chapters; Chapter 2 Related work, Chapter 3 Theory, Chapter 4 Idealized models for power potential, Chapter 5 Power potential from numerical simulations and Chapter 6 Conclusion.

Chapter 2 includes a review of previous studies of theoretical estimates of the power potential of tidal currents. The chapter also includes studies where the power potential has been calculated from data obtained from numerical simulations and then compared to theoretical estimates. In Section 2.1 pre-

vious work done in Rystraumen is presented, this includes the bathymetry of the channel and measurements of the current velocities.

In Chapter 3 the relevant theory necessary to carry out this study is presented. The governing equations describing a tidal current is given, as well as assumptions made to simplify these. The equations are extensively simplified until only one equation describes the evolution of the flow in Rystraumen.

From the last equation given in Chapter 3 the power potential in Rystraumen is estiamted. The importancy of the different terms in the equation is investigated by solving the equation several times: first with the two least important terms of the equation neglected, second with only one term neglected, and at last with all the terms included. The solution of each of these cases is presented together with the estimate of the maximum power potential and a discussion of the results.

To give a more precise estimate of the power potential a numerical model is used to simulate the flow . In Chapter 5 the depth-integrated model used in this study is presented. From the velocity data obtained from the simulations the energy dissipated by the turbines is calculated and an estimate of the maximum extractable energy is given. The result is presented as well as a discussion of the result compared to the results obtained in Chapter 4.

At last, in Chapter 6, the conclusion and suggestions to further work is presented.

Chapter 2

Related work

Exploiting the kinetic energy in a tidal current is far from a new idea. Tidal mills or sea mills have been used for centuries. The Perse mill and the Bacalan mill, both in france, and the Ell Ferol mill in Spain are all examples of energy extraction from tidal currents [Charlier, 2003]. However, recently there has been a growing interest in converting the kinetic energy in a tidal current into electrical energy. Most of the projects are in the early start. The technology for energy extraction from tidal currents is approximately fifteen years behind the wind energy technology [Rourke et al., 2010]. But as there are several similarities between these two technologies, the development of tidal turbines might benefit from this. At the rate the tidal current technology is being developed today, it is expected that within the next ten years full-scale tidal farms will be fully developed [Rourke et al., 2010]. A review of the tidal energy status in 2009 by Rourke et al.(2010) reports that a handful of full-scale single turbines have been successfully tested and are generating electricity [Rourke et al., 2010].

Norway has a long tradition as a sea-nation. The technical principles for energy extraction from a current are already well known, and the concept is more technically mature than other concepts like wave power and offshore wind [Enova SF, 2007]. Still the development of technology is at a very early stage. In Norway, commercial power production is not yet established. There are however several pilot projects, including the Flumill project reviewed in Section 1.2.

Common for all the pilot projects is that they are small scale projects generating power around 1 MW and will therefore have very little impact on

the tidal current [Sutherland et al., 2007]. If the projects become commercialized, several turbines have to be combined into a farm of turbines. Then more energy will be extracted, and the impact on the current flow will be larger. As the interest in tidal stream energy has increased, so has the need for an easy formula to estimate the power potential.

The power potential of a wind turbine is traditionally given as a fraction of the kinetic energy flux. The kinetic energy flux through a cross section A spanned out by turbine blades is given by the following equation:

$$P_{flux} = \frac{1}{2}\rho u^3 A \tag{2.1}$$

where ρ is the density of the fluid and u is the current velocity. The unit for power is watt.

For wind power, Betz law is commonly used and states that the percentage available for extraction is 59 percent of the original kinetic flux of a flow. As the tidal turbines are reminiscent to the wind turbine it is tempting to assume that the power potential of a tidal current might be estimated from the same formula. However, there are some important differences between the wind flow and the flow in a tidal current. Wind turbines extract energy from a thin bottom layer of the atmosphere and therefore allow the flow to recover downstream of the turbine [Bryden et al., 2004].Turbines in a tidal current will extract energy from a significant fraction of the flow, hence one can not assume the flow will recover [Bryden et al., 2004]. This is supported by several studies, which conclude that power potential of a tidal current can not be calculated from the kinetic energy flux [Garrett and Cummins, 2004], [Garrett and Cummins, 2005], ,[Vennell, 2011].

Bryden et al. (2004) have done a theoretical study of the flow through a simple square channel. The study does not lead to any estimation of the power potential, but concludes that energy extraction changes the nature of the flow. Energy extraction reduces the flow speed and hence also the energy flux. If 10% of the kinetic energy flux is extracted, this reduces the current velocity by less than 3%. If the energy extraction is 20% the reduction is approximately 6%. The conclusion from this study is that it is not possible to give an estimate of the power potential based on the energy flux of a natural flow [Bryden et al., 2004].

Several studies have been conducted in order to find a formula for estimating the power potential of a tidal current. Vennel (2011) has developed a sim-

ple method for estimating the power potential of a current with which one needs only knowledge of the bottom friction, the channel dimensions, and the volume transport through the channel.

Garrett & Cummins (2004) have studied the simple case for a tidal current created as the tide flows in and out of a bay through a narrow channel. The difference in surface elevation at each end of the channel, the pressure head, has been assumed to drive the flow. Acceleration of the fluid and natural bottom friction have been ignored. It is also assumed that the velocities at the entrance and exit of the channel are zero. The governing equation has therefore been given as the dynamical balance between the pressure head and the friction force associated with turbines. The friction force has been represented both as a linear friction and quadratic friction. For the linear case the following formula for the maximum power potential was derived:

$$P_{max} = \frac{1}{4}\rho g A \omega a^2 \tag{2.2}$$

where ρ is the density of sea water, g is the gravitational acceleration, A is the surface area of the bay, ω and a is the frequency and amplitude of the tidal constituent given at the entrance of the channel [Garrett and Cummins, 2004]. For the quadratic case the maximum power potential is given as 0.97 times the maximum power potential for the linear case. The quadratic representation of the turbine friction is assumed to be the more realistic representation [Garrett and Cummins, 2004].

Garrett & Cummins (2005) have focused on a channel connecting two larger basins. The basins are so large that the surface elevations are unaffected by the energy extraction in the channel. The governing equation is a balance between the acceleration of the fluid, the pressure head and a friction force. The friction force includes terms for both the natural bottom friction and friction associated with turbines. Three different situations have been discussed, in which the natural friction and the advection term of the momentum equation are of various importance. The result from this study is that the maximum power potential is equal to about 20% to 24% of the peak tidal pressure head times the volume flux through a cross section of an undisturbed current. Even if there is no knowledge about the natural bottom friction, the power potential can still be estimated within 10% from the following formula:

$$P_{max} = 0.22\rho g a Q_{max} \tag{2.3}$$

where ρ is density of sea water, g is gravitational acceleration, a is the difference in amplitude of surface elevation on each end of the channel, and Q_{max} is the volume flux of the undisturbed current [Garrett and Cummins, 2005].

The formula given in Garrett & Cummins (2005) has been tested on real cases. The power potentials have been estimated by the formula derived and the estimations agree reasonably well with the calculations done based on data obtained by numerical simulations [Sutherland et al., 2007]. The studies are however limited to very simple flow situations, and do not apply to the current studied in the present work.

Garrett & Cummins (2008) have once more studied a channel which connects two large basins which are unaffected by the energy extraction. This time the turbine fence only covers a fraction of the channel. Covering the whole cross section with a turbine fence might be in conflict with other interests. A partial turbine fence allows the flow to be diverted around the turbines. Compared to the situation where the turbine fence covers the whole cross section, the power potential is reduced. The study has also accounted for the drag on the supporting structure of the turbine. This is a very important factor, as it will slow down the flow without contributing to the power production. Again the power potential is reduced. Garret & Cummins (2008) have shown that a certain number of turbines will result in a peak in the power potential [Garrett and Cummins, 2008].

Atwater & Lawrence (2010) have studied a situation similar to the one of Garrett & Cummins (2005) where a channel connects two large basins. In this study the channel is split into two sub-channels where energy has been extracted from only one of the sub-channels. The governing equation was given as a balance between the difference in surface elevation and the force caused by resistance due to natural friction, turbine friction and head loss at each end of the channel [Atwater and Lawrence, 2010]. The time dependence is ignored in this study. When the friction associated with turbines is increased in one of the channels, the flow might be diverted to the free channel. To what extent this happens depends on the relative resistance in each sub-channel [Atwater and Lawrence, 2010]. If the natural friction in the free channel was increased to such an extent that no flow passes through, the power potential was the same as for a the single channel situation presented in Garrett & Cummins (2005). If on the other hand the friction in the

free channel approached zero, the power potential was very low. The power potential is therefore not only dependent on the natural flow through the sub-channel where energy is extracted, but also dependent on the relative resistance in each sub-channel [Atwater and Lawrence, 2010].

Sutherland et al. (2007) have evaluated the maximum power potential of Johnstone Strait, Canada, both by the analytic methods presented in Garrett and Cummins (2005) and by a numerical model. They have concluded that for a current flowing through a single channel, the analytic calculations agree reasonably well with the numerical results. For the situation where the channel is branched, and energy only was extracted from one of the sub-channels, the analytic formula was no longer valid, and did not agree with the simulations.

The two most common ways of including the effect of turbines in a numerical model is either as an additional drag term in the momentum equation or as an additional loss in the energy equation [Defne et al., 2011, Sutherland et al., 2007]. In the study done by Sutherland et al. (2006) the drag effect from the turbines has been included by increasing the bottom friction in the areas where the turbines are located. The same method has been used in the study by Plew & Stevens (2013) to estimate the power potential in Tory Channel, New Zealand. They have used a two-dimensional depth integrated finite element model to decide the power potential and the effect of arrays of turbines. However, the additional stress includes both the turbine thrust and the structural drag.

Also in the study done by Draper et al. (2014) the turbine drag has been introduced as an additional stress term in the depth-averaged numerical model. They have estimated the power potential of the Pentland Firth, Orkney Island. The channel consists of several sub-channels and the effect of energy extraction from one or several of these sub-channels has been investigated. One of the results is that the location of the turbine arrays affects the extraction in other sub-channels and the overall power potential. The highest value for power potential was obtained if the turbine fences covered the whole width of the Pentland Firth [Draper et al., 2014].

As mentioned in several studies, the introduction of turbines in a current might change the flow pattern, both locally and in distance from the extraction point. Change in the overall flow pattern may change the transport of sediments and nutriciant, and suspended material [Sutherland et al., 2007, Plew and Stevens, 2013].

2.1 Former research in Rystraumen

In the Northern Sea, the tidal wave comes partly through the English channel and partly from the north and causes interference [Grabbe et al., 2009]. As Grabbe et al. (2009) state in their study, this gives large tide differences at some locations, while other places are more or less unaffected. The tide variation along the coast of southern Norway is very small but from the west coast and in northern direction the variation increases [Grabbe et al., 2009]. In the Vestfjord, the fjord between the Lofoten islands and the mainland, the variation is as large as 3.6 meters [Grabbe et al., 2009]. North of this, in Vesterålen, the variation is smaller. The strong currents between the Lofoten Islands may explain this. Further north, the tidal variation increases again: in Vardø the variation is as large as in Vestfjorden [Grabbe et al., 2009]. Even though the variation of water level is large all the way from the west coast to Bodø, there are no narrow straits going in such a direction that the tidal change creates a strong current [Grabbe et al., 2009].

The tidal current in Rystraumen is created by the large difference in high tide and low tide in the northern part of Norway, close to Tromsø. The flow associated with ebb and flood is funneled as it moves through a straight between the two islands Kvaløya and Ryøya and the mainland. The current at its maximum exceeds 3 m/s and is therefore highly suitable for energy extraction [Enova SF, 2007, Grabbe et al., 2009, Flumill, 2011].

As a part of the preparation for the Flumill project a mapping of the seafloor and measurements of the velocities of the current has been conducted. Mapping of the sea floor was done by Geonord Survey Team in 2012 using sidescan sonar. The survey was made in order to decide what the seabed consisted of and in order to do a bottom classification. In the sidescan survey report (2013) it is stated that the sea floor in the relevant area is mainly flat, but that it also has wave formations indicating a seabed covered by sediments. These formations were especially evident in the areas where the channel becomes wider and the current velocity decreases [GeoNord Survey Team, 2013]. In the middle of the channel the depth varies from 60 to 70 meters, see Figure 2.2. The channel walls are steep and consist of hard rock [GeoNord Survey Team, 2013].

Measurements of the current velocity in Rystraumen were done by Aquatera Ltd in 2012 and were presented in an addendum to the Sidescan survey report done by GeoNord. Current data were collected with a vessel mounted Acoustic Doppler Current Profiling (ADCP) ocean surveyor. This type of

Figure 2.1: The current Rystraumen is a narrow strait located in the north of Norway, just outside Tromsø [Google, 2014].

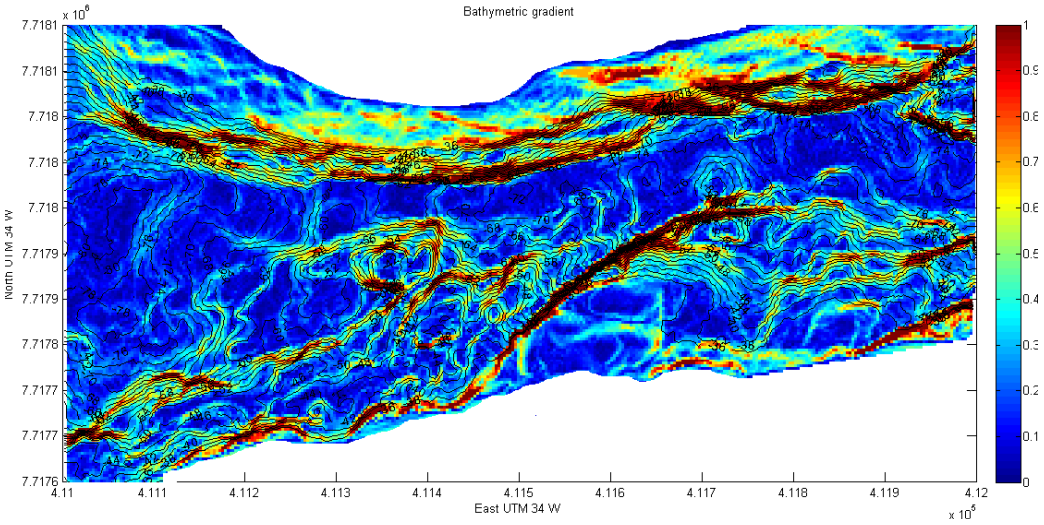

Figure 2.2: Bathymetric data collected by Geonord Survey Team. A gradient of 1 corresponds to a slope of 100 percent or 45 degrees [GeoNord Survey Team, 2013].

measurement is ideal for depths of less than 100 meters with an estimated error of less than 0.5 % [Aquatera Ltd, 2013].

The area focused on is between the island Kvaløya, the small island Ryøya and the mainland. 13 hours of continuous measurements were done with eight tracks crossings the straight with a hundred meters distance Figure 2.3 [Aquatera Ltd, 2013]. The measurements were done from 5 meters below still water level and down to a few meters above the seabed.

The mean spring tidal range is 2.1 meters in Rystraumen, at the time the measurements were done the tidal range was 1.45 meters. In the report from Aquatera Ltd a linear relationship between the current velocities and the tidal range has been assumed. This has been used to scale up the velocities to find the mean spring peak current velocity. So as $2.1/1.45 \approx 1.45$, the measured velocities in the following figures have been multiplied with 1.45. The maximum velocity of 2.5 m/s was measured 5 meters below the surface, which gives a near surface peak velocity as high as 3.6 m/s [Aquatera Ltd, 2013].

The installations will be placed at a depth of 60-75 meters. Therefore the measurements done at 45 meters below surface were chosen, as this is where the energy will be harvested [Aquatera Ltd, 2013]. The report suggests that the areas best suited for energy extraction are the central parts of the channel. At 45 meters deep these central parts are where the highest velocities were found. Based on these measurements and calculation of peak currents, three

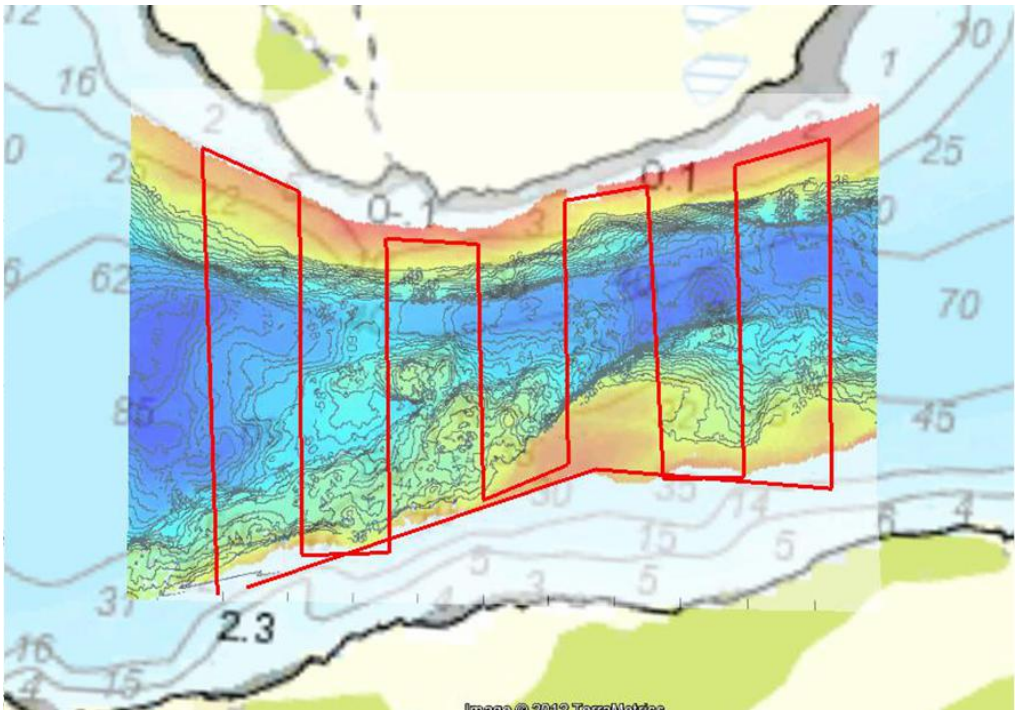

Figure 2.3: The eight tracks covering the area in Rystraumen by the ADCP ocean surveyor [Aquatera Ltd, 2013].

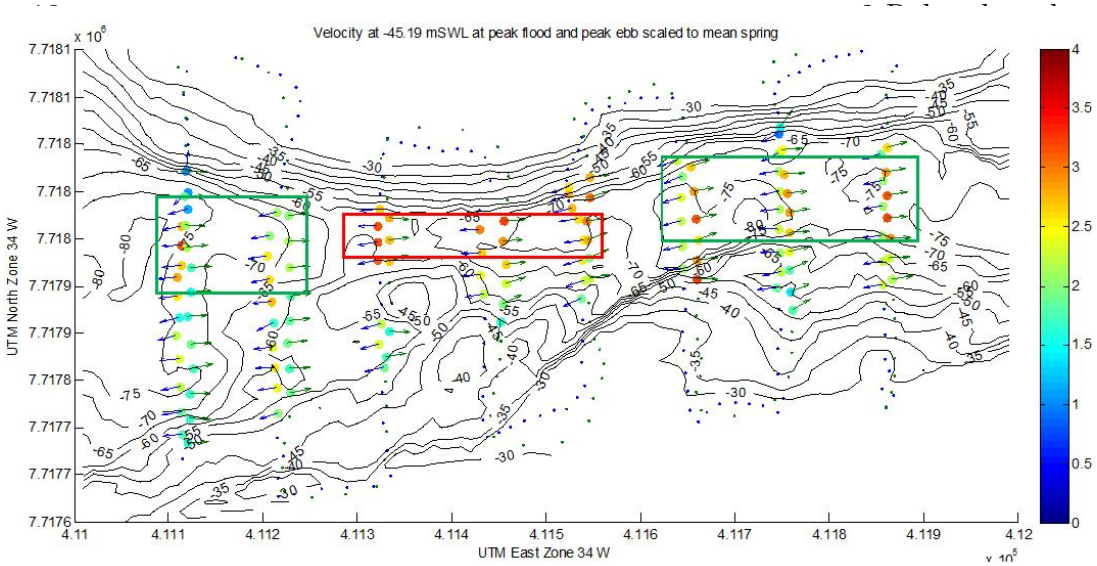

Figure 2.4: Peak ebb and flood mean spring velocity at 45 meters depth in Rystraumen [Aquatera Ltd, 2013].

main areas where selected as highly relevant for the pilot project, as shown in figure 2.4. Two of the areas (within green marking) had a significant current velocity in just one direction [Aquatera Ltd, 2013]. The third area (within the red marking) had significant current velocity in both directions [Aquatera Ltd, 2013]. Eight areas within the red marking have been pointed out as suitable for tidal turbine devises, as the bottom slope in these areas is less than 10% [Aquatera Ltd, 2013]. In addition, a shallower area with very high velocities has been pointed out in the south of the channel. This might be a good area for testing of shallow water devises.

Chapter 3

Theory

In this chapter the theory, which the methods used in this study are based upon, is presented. A set of governing equations is presented in Section 3.1 which will be further developed and used in both Chapter 4 and Chapter 5. The depth integrated version of these equations make up the model from which the flow in Rystraumen is simulated (Chapter 5). In this chapter the equations given in Section 3.1 will be simplified until the flow of Rystraumen can be described by one single governing equation. From this single equation the estimates of the power potential in Rystraumen is calulated (Chapter 4).

3.1 The governing equations

The evolution of the flow in a tidal current is described by the velocity vector and the pressure in the following governing equations:

$$\nabla \cdot \boldsymbol{V} = 0 \tag{3.1}$$

$$\frac{Du}{Dt} + \frac{1}{\rho}\frac{\partial p}{\partial x} - fv = \mathcal{F}_x \tag{3.2}$$

$$\frac{Dv}{Dt} + \frac{1}{\rho}\frac{\partial p}{\partial y} + fu = \mathcal{F}_y \tag{3.3}$$

$$\frac{1}{\rho}\frac{\partial p}{\partial z} + g = 0 \tag{3.4}$$

where $\boldsymbol{V}$ is the velocity vector, u and v are the x- and y-component of the velocity, p is the pressure, f is the Coriolis parameter, $\mathcal{F}_x$ and $\mathcal{F}_y$ represent the frictional forces in x- and y-direction respectively and g is the gravitational acceleration [Marshall and Plumb, 2008].

3.1 is the continuity equation, while 3.2, 3.3 and 3.4 are the x, y and z components of the momentum equation, also referred to as the Navier-Stokes equations [Tu et al., 2008]. These four equations in addition to the boundary conditions give a closed system of equations which describes the flow of the tidal current.

In addition to the four variables mentioned, also temperature and salinity are variables describing an ocean flow. These variables are however not considered to be crucial for the flow features of a tidal current, and their contribution to the flow pattern has been neglected. The fluid is considered to have a uniform density.

The general continuity equation is derived from mass conservation. Given a control volume dV the change in mass over a time dt has to equal the mass going out of or entering the control volume through the control surfaces dS [Garg, 1998]. Water can, for most dynamical purposes, be considered as an incompressible fluid and the continuity equation is reduced to the one given in 3.1 [Marshall and Plumb, 2008].

The equations for motion, 3.2, 3.3 and 3.4, are derived from Newton's second law [Tu et al., 2008]. The sum of forces working on a fluid parcel has to equal the acceleration of the parcel times its mass. Forces working on a fluid are often divided between forces working on the whole body of the parcel, referred to as body forces, and forces working on the surface of the fluid parcel, referred to as surface forces. The body forces are due to gravitation, Corilolis effect and the centrifugal effect while the surface forces are frictional forces and forces due to pressure gradients [Tu et al., 2008].

For a flow of sea water one can neglect the frictional force everywhere, except close to the boundaries [Marshall and Plumb, 2008]. Along the sea bottom irregularities will increase the rate of momentum diffusion. At the sea surface the wind will stir up the water surface and create turbulence and enhance the momentum exchange between sea and air [Marshall and Plumb, 2008].

The friction along the boundaries is included in the friction terms $\mathcal{F}_x$ and $\mathcal{F}_y$ which also will include the friction associated with turbines.

The pressure force working on each surface area of a fluid parcel is given as the pressure times the area of the surface [White, 2011]. The pressure gradient is the difference in pressure on two opposing surfaces, and is given as components for the x, y and z- directions in the three momentum equations.

The gravitational acceleration only has a component in z-direction, and will therefore only contribute to the z-component of the momentum equation [Marshall and Plumb, 2008]. In Rystraumen the sea floor gradient will be very small, hence there will only be a small vertical acceleration. The acceleration term of the vertical velocity w, including the advection term $\boldsymbol{V} \cdot \nabla w$, is zero, hence also the z-component of the friction. The z-component of the momentum equation is therefore reduced to hydrostatic pressure.

For Rystraumen, it might be discussed whether or not it is realistic to neglect the acceleration of the vertical velocity. For a large scale oceanic system the vertical motion is small [Marshall and Plumb, 2008]. However in Rystraumen the steep walls on each side might create a vertical motion large enough to affect the flow. On the other hand, the main direction of the fluid flow is along the channel, and not across it, and therefore in this study it is reasonable to assume hydrostatic pressure.

The fluid is described in a coordinate system rotating with an angular velocity Ω. When Newton's Second Law is considered, the acceleration term has to include both the acceleration of the fluid element relative to the earth and the acceleration due to the earth's rotation. The latter gives rise to the centrifugal effect and the Coriolis effect. As will be explained, these effects play a major role in the dynamics of the large oceans, however on smaller scale these effects are of less influence [Marshall and Plumb, 2008].

The centrifugal effect results in an additional acceleration pointing outwards from the axis of the rotation and modifies the gravitational acceleration. The centrifugal acceleration a_c, which can be included in the gravitational acceleration, is given as

$$a_c = \Omega^2 R cos(\varphi) \tag{3.5}$$

where Ω is the angular velocity of the earth, R is the radius and φ is the latitude [Marshall and Plumb, 2008]. As the cosine function will equal one at

the equator, the centrifugal force will be strongest here and decreasing toward the poles. The earth rotates 2π radians over an period of 86 400 seconds, this gives an angular velocity $\Omega = 7.27 \cdot 10^{-5} rad/s$. R is the sum of the radius of the earth r and the depth of the sea D [Marshall and Plumb, 2008]. However, as the depth of the sea is much smaller than the radius of the earth, it is reasonable to assume that $R \approx r$, where $r = 6371km$. At the longitude $\varphi = 69°$, where Rystraumen is located, the centrifugal acceleration $a_c = 1.2 \cdot 10^{-2} ms^{-2}$. This is about one hundred times smaller than the gravitational acceleration and therefore the centrifugal acceleration of the flow in Rystraumen can be neglected.

The Coriolis parameter f is given by:

$$f = 2\Omega sin(\varphi) \tag{3.6}$$

where the variables Ω and φ are given as for the centrifugal acceleration [Marshall and Plumb, 2008]. To decide whether or not the Coriolis term is of importance for the evolution of the flow the Rossby number can give an indication. The Rossby number is given as the ratio of the advection term on the Coriolis term:

$$Ro = \frac{|\boldsymbol{V}|}{Lf} \tag{3.7}$$

where $|\boldsymbol{V}|$ is the magnitude of the velocity vector, L is the length of the channel and f is the Coriolis parameter given in 3.6 [White, 2011]. In Rystraumen $L = 2000m$, the velocity at its maximum $|\boldsymbol{V}| = 3m/s$ and $f = 1.36 \cdot 10^{-4} s^{-1}$, the Rossby number equals 11. The advection term is therefore ten times larger than the Coriolis term, so the Coriolis acceleration in Rystraumen can be neglected.

3.2 Reduction to one governing equation

To be able to easily give an estimate of the power potential of a tidal current, the governing equations needs further simplifications.

As mentioned, the vertical acceleration in a channel might be neglected due to the small gradients of the sea floor. For Rystraumen the main transport is

in x-direction, assuming the x-axis is aligned with the length of the channel. The y-component of the velocity is small compared to the one in x-direction. This allows us to neglect the velocity in y-direction as well as the acceleration of v. As seen in Figure 2.2, the only steep gradients in Rystraumen are in y-direction, along the walls of the channel. However, if the y-component of the velocity is neglected, than there will not be any acceleration of the velocity in this direction either, and the velocity w will be small compared to the x-component of velocity. When the acceleration of v and w have been neglected, the friction terms in the same direction disappear too. The Coriolis term has already been neglected for a current in a channel, so the governing momentum equations are simplified to the following:

$$\frac{\partial u}{\partial t} + u\frac{\partial u}{\partial x} + \frac{1}{\rho}\frac{\partial p}{\partial x} = \mathcal{F}_x \tag{3.8}$$

$$\frac{1}{\rho}\frac{\partial p}{\partial y} = 0 \tag{3.9}$$

$$\frac{1}{\rho}\frac{\partial p}{\partial z} = g \tag{3.10}$$

To be able to give a quick estimate of the power potential of a current I want to describe the flow by one single equation. To achieve this, 3.8 is integrated over the cross sectional area of the channel. The integration has been done by applying Leibniz' integral rule twice; first on the integral over the width and then on the integral over the depth.

The average velocity over the cross sectional area of the channel has been defined to

$$\overline{u} = \frac{1}{A}\int_{-H}^{\zeta}\int_{W_1}^{W_2} u dy dz \tag{3.11}$$

and the average velocity over the width of the channel is defined to

$$\widetilde{u} = \frac{1}{\Delta W}\int_{W1}^{W2} u dy \tag{3.12}$$

where A is the cross sectional area of the channel, H is the depth of the channel, ζ is the surface elevation and W_1 and W_2 denote the horizontal channel boundaries, the channel walls. All these sizes are functions of x as the cross sectional area might vary along the length of the channel.

When integrating the first term in 3.8 twice the following is obtained:

$$\int_A \frac{\partial u}{\partial t} dA = A\frac{\partial \overline{u}}{\partial t} + \int_{-H}^{\zeta} \left(\widetilde{u(W_2)} \frac{\partial W_2}{\partial t} - \widetilde{u(W_1)} \frac{\partial W_1}{\partial t} \right) dz + \widetilde{u(\zeta)} \frac{\partial \zeta}{\partial t} \Delta W - \widetilde{u(-H)} \frac{\partial (-H)}{\partial t} \Delta W \quad (3.13)$$

where $\Delta W = W_2 - W_1$. The second, third and fifth term are zero as the channel dimensions obviously do not change with time, thus

$$\int_A \frac{\partial u}{\partial t} dA = A\frac{\partial \overline{u}}{\partial t} + \widetilde{u(\zeta)} \frac{\partial \zeta}{\partial t} \Delta W \quad (3.14)$$

The average velocity squared over the cross sectional area of the channel is defined as

$$\overline{u}^2 = \frac{1}{A} \int_{-H}^{\zeta} \int_{W_1}^{W_2} u^2 dy dz \quad (3.15)$$

and the average velocity squared over the width of the channel is defined as

$$\widetilde{u} = \frac{1}{\Delta W} \int_{W1}^{W2} u dy \quad (3.16)$$

Integrating the advection term over the cross sectional area gives the following equation

$$\int_A \frac{\partial u^2}{\partial x} dA = A\frac{\partial \overline{u}^2}{\partial x} + \int_{-H}^{\zeta} \left(\widetilde{u(W_2)}^2 \frac{\partial W_2}{\partial x} - \widetilde{u(W_1)}^2 \frac{\partial W_1}{\partial x} \right) dz + \widetilde{u(\zeta)}^2 \frac{\partial \zeta}{\partial x} \Delta W - \widetilde{u(-H)}^2 \frac{\partial (-H)}{\partial x} \Delta W \quad (3.17)$$

Assuming no-slip condition where the velocity along the channel walls and bottom is zero, the second, third and fifth term disappear. The velocity at the surface is not zero. The advection term now consists of the advection of the average velocity and the squared velocity at the surface times the gradient of the surface elevation:

$$\int_A \frac{\partial u^2}{\partial x} dA = A\frac{\partial \overline{u}^2}{\partial x} + \widetilde{u(\zeta)}^2 \frac{\partial \zeta}{\partial x} \Delta W \tag{3.18}$$

An expression for pressure can be derived from the 3.10. By integrating this equation from the depth $-z$ to ζ the following is obtained

$$P_a - P(z) = \rho g(\zeta - z) \tag{3.19}$$

where P_a is the atmospheric pressure and $P(z)$ is the hydrostatic pressure which increases with the depth. Derivating the pressure term with respect to x and t, gives an expression for the pressure gradient in 3.8. The atmospheric pressure is not important for a tidal flow, hence we set the derivate equal to zero. Also the depth z derivated with respect to x is zero, leaving the pressure gradient term independent of z. The pressure gradient is now expressed as a derivate of the surface elevation times the gravitational acceleration:

$$\frac{1}{\rho}\frac{\partial p}{\partial x} = g\frac{\partial \zeta}{\partial x} \tag{3.20}$$

As the acceleration of v is neglected in 3.9 the pressure gradient in y-direction equals zero, and the pressure is independent of y. As the pressure gradient is only a function of x, the integral over the cross sectional area becomes:

$$\int_A g\frac{\partial \zeta}{\partial x} dA = g\frac{\partial \zeta}{\partial x} A \tag{3.21}$$

Dividing the whole equation by $A = D\Delta W$ the flow evolution is now described by the following single momentum equation:

$$\frac{\partial \overline{u}}{\partial t} - \frac{1}{D}\widetilde{u(\zeta)}\frac{\partial \zeta}{\partial t} + \frac{\partial \overline{u}^2}{\partial x} - \frac{1}{D}\widetilde{u(\zeta)}^2(\zeta)\frac{\partial \zeta}{\partial x} + g\frac{\partial \zeta}{\partial x} = \mathcal{F}_x \tag{3.22}$$

3.2.1 Scaling of the governing equation and further simplifications

The terms in 3.22 is of various importance. To decide which of them are crucial for describing the flow, the terms are scaled and compared to each other. All the quantities here is given as approximate values for Rystraumen to give the order of the terms in 3.22.

The first term can be considered as the change in the current velocity over a tidal period.

$$\frac{\partial \overline{u}}{\partial t} \approx \frac{\Delta U}{\Delta T} \tag{3.23}$$

The tidal current flows in one direction for 6 hours, before it changes direction. Over these 6 hours the maximum velocity will increase from 0 to $3m/s$ over the first three hours, before it decreases to zero for the next three hours. If the maximum average velocity in the current is assumed to vary with $\Delta U = 1m/s$ over a period of 3 hours, $\Delta T = 10800s$, the first term is of order $10^{-4}m/s^2$.

The second term is given as the velocity divided by the depth times the change in surface elevation over time:

$$\frac{\widetilde{u}}{D}\frac{\partial \zeta}{\partial t} \approx \frac{U}{D}\frac{\Delta \zeta}{\Delta T} \tag{3.24}$$

The average current velocity $U = 1m/s$, and the average depth over a cross section of the channel is $D \approx 40m$. The difference in surface elevation in Rystraumen over a 6 hour period, $\Delta T = 21600s$, is $\Delta \zeta \approx 2m$, so second term is of order $10^{-6}m/s^2$.

The third and the fourth term are derived from the advection term. The third term is scaled as following

$$\frac{\partial \overline{u}^2}{\partial x} \approx \frac{\Delta U^2}{L} \tag{3.25}$$

where the length of the channel $L = 2000m$. For Rystraumen, the flow of water in eastern direction entering the channel, is drawn from a large

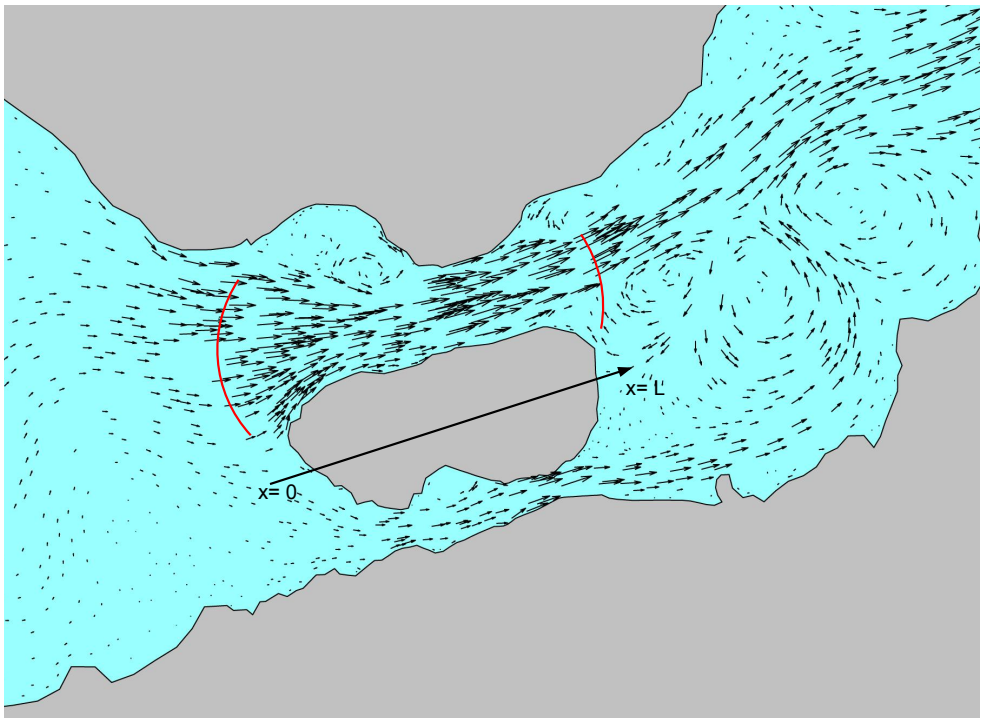

Figure 3.1: Quiver plot of Rystraumen for flow in eastward direction. The entrance and the exit of the channel is indicated with the red lines. The arrow aligned with the channel indicates the x-axis where the entrance is at x=0 and the exit at x=L (FVCOM simulations).

basin with a large cross section. For a constant volume flux this means that the velocity at the entrance is zero. At the exit of the channel, when the current already has obtained a certain velocity, it is reasonable to assume that it will take a while before the current velocity is reduced to zero. The flow pattern is shown in a quiver plot of Rystraumen in Figure 3.1. If the average velocity out of the channel is $U \approx 1m/s$ the advection term equals $5 \cdot 10^{-4} m/s^2 \approx 10^{-3} m/s^2$. The velocity given here is an approximate value and it is worth mentioning that if this value is less than what is given here, the order of the term is $10^{-}4m/s^2$.

The fourth term:

$$\frac{\widetilde{u(\zeta)}^2}{D}\frac{\partial \zeta}{\partial x} \approx \frac{U^2}{D}\frac{\Delta \zeta}{L} \tag{3.26}$$

where the velocity is given as the maximum velocity $U \approx 1m/s$, $D = 40m$,

$L = 2000m$ and the change in surface elevation across the length of the channel is less than a meter. When $\Delta\zeta = 0.5m$, the term is of order $10^{-5}m/s^2$.

The fifth term derived from the pressure gradient is the driving force of the flow and can be scaled as:

$$g\frac{\partial\zeta}{\partial x} \approx g\frac{\Delta\zeta}{L} \tag{3.27}$$

where $\Delta\zeta$ and L is given as before and $g = 9.81m/s^2$. The term is of order $10^{-3}m/s^2$ and therefore thousand times larger than the smalles term and ten times larger than the second largest term on the left side of the 3.22. Different representation of the friction term will be introduced in Chapter 4 and therefore this term is not scaled here.

By neglecting the terms of the lowest order, the second and the fourth term, the 3.22 is reduced to the following governing equation for a flow in a channel with varying cross sectional area:

$$\frac{\partial\overline{u}}{\partial t} + \overline{u}\frac{\partial\overline{u}}{\partial x} + g\frac{\partial\zeta}{\partial x} = -F \tag{3.28}$$

Also the first term, the time derivative is ten times smaller than the advection term and the pressure gradient and might therefore be neglected. However, the term has been included in the work done by Garrett & Cummins (2005) and therefore kept for further investigation also in this work.

Chapter 4

Idealized models for power potential

In this chapter equation 3.28 is investigated further to give an estimate of the power potential of Rystraumen and to decide which of the terms in the equation are more important for a precise estimate.

In the following Section 4.1 the two first terms in 3.28 are neglected and the maximum power potential is decided from an equation balanced by the pressure gradient and the resistance due to turbine friction. The equation given in this section is solved for the case where the turbine friction is given to be linearly proportional to the current velocity and for the case when this relationship is given to be quadratic.

In Section 4.2 the time derivative of the velocity is included, and the balance in the equation is now between this term, the pressure gradient and the turbine friction. Also this equation is solved for both linear and quadratic turbine friction representaion.

Finally in Section 4.3 the last term in 3.28, the advection term, is included. The system of equations obtained in this section is only solved for quadratic friction.

All the constants for Rystraumen is given in Table 4.1 for all the following cases.

Constant		
A	Cross sectional area of channel	$19474m^2$
A_B	Surface area of Balsfjord	$268790000m^2$
L	Length of channel	2000m
ρ	Density of sea water	$1025kg/m^3$
g	Gravitational acceleration	$9.81m/s^2$
a	Amplitude of M2	1m
ω	Frequency of M2	$2\pi/(12 \cdot 3600s + 25.5 \cdot 60s)$

Table 4.1: Constants calculated from the model grid

4.1 Balance between pressure gradient and turbine friction

The starting point of this chapter is 3.28. According to the scaling done in Section 3.2 the most important terms in the equation is the pressure gradient and the friction term. By neglecting the two smallest terms, the time derivate of the velocity and the advection term, the flow is now described by a balance between the pressure gradient and the force associated with friction:

$$g\frac{\partial \zeta}{\partial x} = -\mathcal{F}_x \tag{4.1}$$

The equation is integrated over the length of the channel

$$g(\zeta_B - \zeta_0) = -\int_0^L \mathcal{F}_x dx \tag{4.2}$$

where $x = 0$ is the entrance of the channel, $x = L$ is the exit and ζ_0 and ζ_B are the surface elevation at $x = 0$ and $x = L$ respectively.

The basin on the outside of the channel is so large that it is reasonable to assume that the surface elevation ζ_0 is unaffected by the energy extraction. For simplicity only the most dominant tidal constituent, M_2, is considered and the surface elevation is therefore given by

$$\zeta_0 = acos(\omega t) \tag{4.3}$$

where a is the amplitude and ω is the frequency.

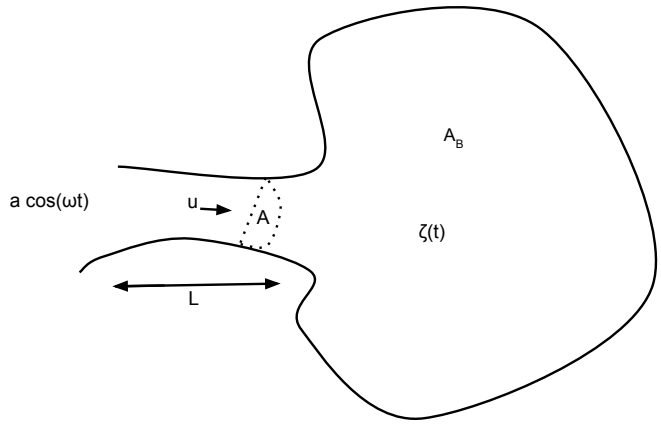

Figure 4.1: Schematic of a tidal current created as the tide flows in and out of a bay through a channel.

The surface elevation in Balsfjord and in the sea east of Rystraumen, ζ_B, is mainly due to the flux of water through Rystraumen and will therefore not be unaffected by energy extraction. ζ_B is therefore an additional unknown in 4.2. If one for simplicity assumes that the volume flux passing around the island Tromsø is small compared to the volume flux through Rystraumen, then Balsfjord and the sea between Balsfjord and Tromsø can be viewed as a closed pool where Rystraumen is the only connection to the rest of the sea. This is illustrated in Figure 4.1. Assuming that the surface elevation ζ_B in this pool, hereafter referred to as Balsfjord, is uniform over the whole pool the following equation is given from mass conservation:

$$A_B \frac{d\zeta_B}{dt} = Au \tag{4.4}$$

where A_B is the surface area of the pool, A is the cross sectional area of the channel and u is the current velocity. If the channel is short compared to the wave length of the tide the volume flux is constant along the channel and can be written as $Au = Q(t)$ [Garrett and Cummins, 2005].

Linear turbine friction

If the turbine friction is assumed to be linear proportional to the current velocity, the force associated with the turbines can be given as in Garrett & Cummins (2005):

$$\int_0^L \mathcal{F}_x dx = \lambda_L Q \tag{4.5}$$

where λ_L is a coefficient related to the number of turbines and has the unit $(ms)^{-1}$. Similar to Garrett & Cummins (2004) the natural background friction is neglected for simplicity.

Inserting 4.5 and 4.4 into 4.2 gives the following differential equation:

$$\frac{\partial \zeta_B}{\partial t} = \frac{g}{\lambda_L A_B} \left(acos(\omega t) - \zeta_B\right) \tag{4.6}$$

where the constants are given in Table 4.1. The equation is solved numerically in matlab with the solver ode15s for stiff differential equations. This solver was chosen as the solver for nonstiff differential equations was slow. The equation was solved for an increasing λ_L and this solver gave the smoothest graph. The result is presented in Figure 4.2 and shows how the volume flux decreases as more energy is dissipated with increasing friction.

The power potential is calculated from the average squared volume flux

$$P = \lambda_L \rho \overline{Q^2} \tag{4.7}$$

where ρ is the density of salt water and given in Table 4.1. The overbar indicates the average over one tidal cycle [Garrett and Cummins, 2005]. The result is presented in Figure 4.3. At first the power is increasing as λ_L is increasing, before the power starts decreasing. As λ_L is increased the flow experiences more resistance, and at a certain point the velocity is so much reduced that the power, which is proportional to the volume flux squared, decreases. The maximum power potential is 95 MW and is achieved when the average volume flux in Rystraumen is reduced to 17 010 m^3/s.

In Garrett & Cummins (2004) the formula

$$P_{max} = \frac{1}{4} \rho g A_B \omega a^2 \tag{4.8}$$

has been derived from the same equations presented in this section for linear friction. Inserting the constants given in Table 4.1, $P_{max} = 95MW$, which agrees with the results obtained in this study for linear friction.

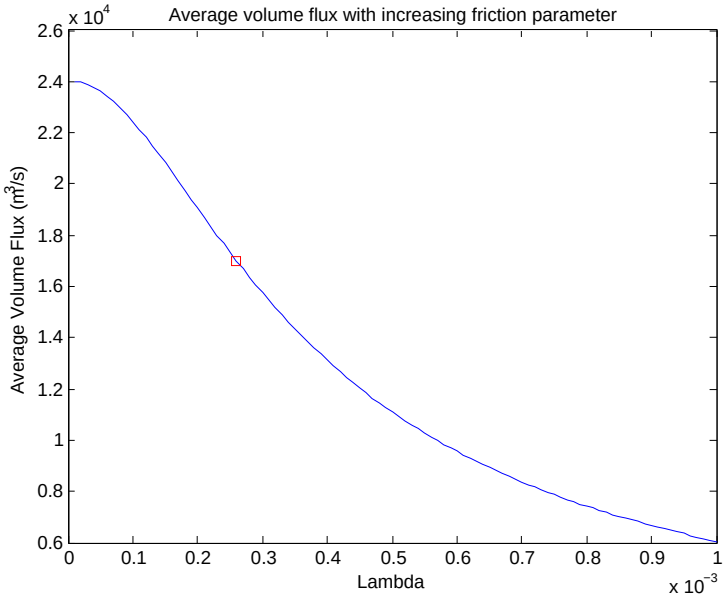

Figure 4.2: Average volume flux calculated from 4.6, with a balance between the pressure gradient and the resistance due to linear friction, for an increasing λ_L. The red square indicates the average volume flux when maximum power potential is reached. This is given in Figure 4.3

Both the result obtained from 4.6 and the formula given in 4.8 are expected to overestimate the maximum power potential. The two terms left out, especially the advection term will lower the power potential. If theese terms are included some of the energy which in 4.6 was available for energy extraction, will go to acceleration of the flow instead and a lot of the energy will be transported out of the channel with the flow as the current exceeds the channel length. Also the background friction has been neglected, but in reality some of the energy in the flow will be dissipated along the channel bottom and walls.

Another factor which will affect the result obtained here is a more realistic representation of the turbine drag as quadratic dependent of the velocity [Garrett and Cummins, 2005].

Quadratic Friction

For quadratic friction the force associated with turbine friction is given as

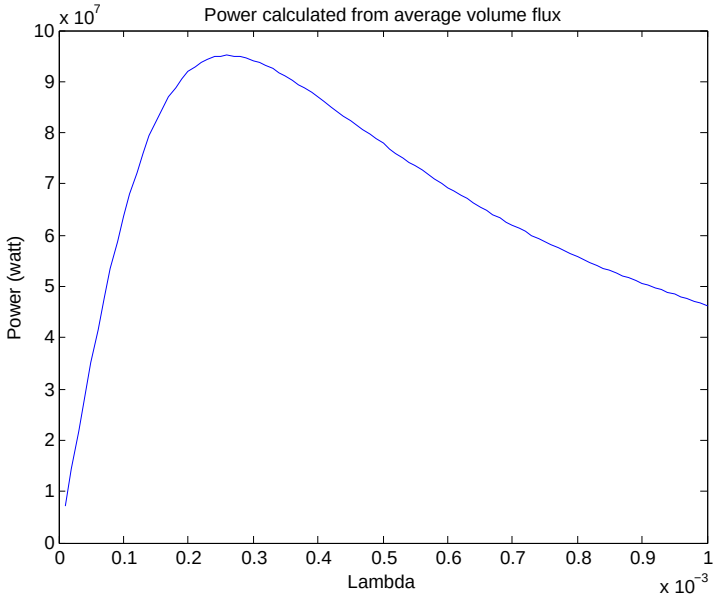

Figure 4.3: Power calculated from 4.7. The volume flux is calculated from 4.6. The turbine friction is linearly dependent on the velocity.

$$\int_0^L \mathcal{F}_x dx = \lambda_S |Q| Q \tag{4.9}$$

where λ_S again is related to the size and number of turbines, but different from the linear case, the unit is now m^{-4}.

Inserting the quadratic representation of the friction term 4.9 and 4.4 into 4.2 gives the following differential equation:

$$\frac{\partial \zeta_B}{\partial t} = \sqrt{\frac{g}{\lambda_S}} \frac{1}{A_B} \sqrt{\left| acos(\omega t) - \zeta_b \right|} sign(acos(\omega t) - \zeta_B) \tag{4.10}$$

where the constants are given in Table 4.1. To preserve the direction of the time derivative of ζ_B, the equation has been multiplied with the sign of the expression inside the square root. The equation is solved numerically in matlab with the same solver used for the linar case above. The average volume flux for increasing turbine friction λ_S is presented in Figure 4.4.

The power is calculated from the following equation

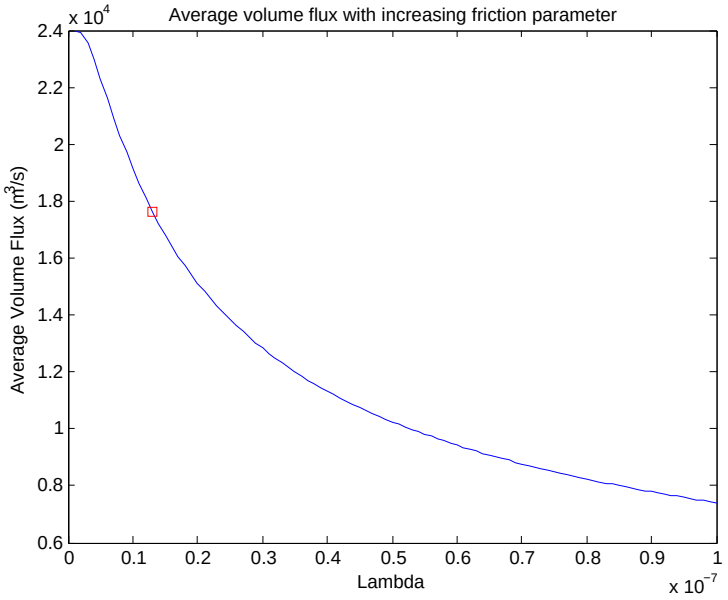

Figure 4.4: Average volume flux calculated from 4.10 with a balance between the pressure gradient and the resistance due to quadratic friction, for an increasing λ_S. The red square indicates the average volume flux when maximum power potential is reached, this is given in Figure 4.5

$$P = \lambda_S \rho \overline{Q^3} \tag{4.11}$$

As can be seen from Figure 4.3 and Figure 4.5 λ_S for the quadratic representation of the turbine friction is of order 10^{-4} times smaller than λ_L for the linear case. This can be explained from the different power formulas 4.7 and 4.11. For the linear case the power is proportional to the volume flux squared, which is of order $(10^4)^2$, while the power for the quadratic case is proportional to the volume flux cubed and is of order $(10^4)^3$ and therefore are 10^4 larger. For the power obtained from the two formulas 4.7 and 4.11 to give an answer of the same order, λ_S has to be correspondingly smaller than λ_L.

The power potential is calculated for an increasing λ_S and is presented in Figure 4.5. Again it is seen that the power potential increases until it reaches a certain λ_S, and then it decreases. The maximum power potential for quadratic turbine friction is 93 MW and is achieved when the average volume flux is reduced to 17 639 m^3/s.

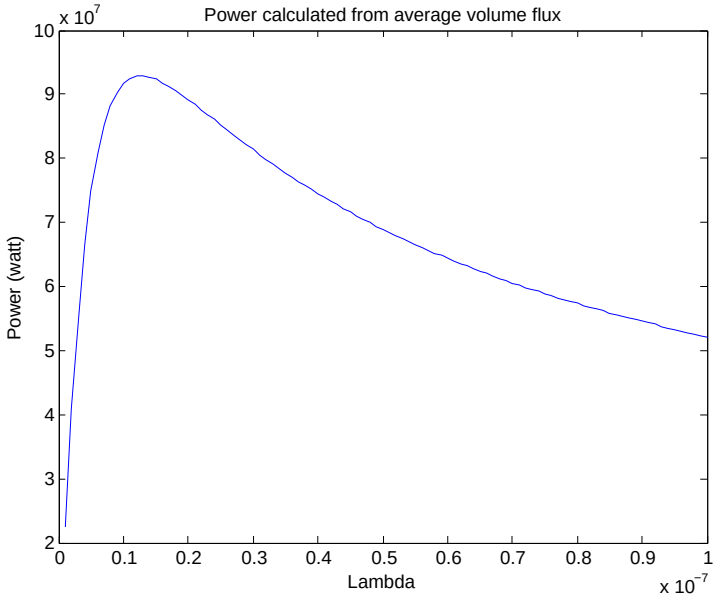

Figure 4.5: Power calculated from the 4.11 where the volume flux is calculated from 4.10 where the turbine friction is quadratic proportional to the velocity.

The maximum power potential for quadratic friction is 0.98 times the maximum power potential calculated for the linear turbine friction. In Garrett & Cummins (2004) the maximum power potential calculated with quadratic turbine friction is $0.97P_{max}$, where P_{max} is derived from linear friction and given in Equation 4.8.

Still, the estimate for power potential given here, is expected to be overestimated because of the terms left out from the 3.28 and because the background friction is not included. In the next section the time derivative, which has been neglected until now, will be included.

4.2 Balance between time derivative of velocity, pressure gradient and turbine friction

Back to 3.28 where only the advection term is neglected this time. From the solutions obtained in this section it will be possible to decide the importance of the time derivate of the velocity.

Again, as in Section 4.1, it is assumed that the channel length is short compared to the wave length of the tide, so that the volume flux is constant through Rystraumen and is given by $Q(t)) = Au$, where A is the cross sectional area of the channel and u is the current velocity. Substituting this into the time derivative term in 3.28, the following equation is obtained:

$$\frac{1}{A}\frac{\dot{\mathrm{Q}}}{dt} + g\frac{\partial \zeta}{\partial x} = \mathcal{F}_x \tag{4.12}$$

where the balance now is between the time derivative, the pressure gradient and the resistance due to turbine friction.

The equation has been integrated along the channel length to give the following:

$$\frac{dQ}{dt}\int_0^L \frac{1}{E}dx + g\left(\zeta_B - \zeta_0\right) = -\int_0^L \mathcal{F}_x dx \tag{4.13}$$

where $x = 0$ is the entrance of the channel and $x = L$ is the exit, ζ_0 is the surface elevation in the basin outside the channel, and ζ_B is the surface elevation on the east side of the channel. As for Section 4.1 the surface elevation ζ_0 in the large basin is unaffected by energy extraction and is given as the M2 tidal constituent where $\zeta_0 = acos(\omega t)$. The surface elevation ζ_B at the other end of the channel is not unaffected by energy extraction from the current. The relationship between the surface elevation ζ_B and the volume flux through Rystraumen is given by 4.4.

The natural friction along the bottom and channel walls is neglected for both the linear case and the quadratic case following and the term $\mathcal{F}_x$ represents only the turbine friction.

Linear Friction

As a start the turbine friction is assumed to be linearly proportional with the current velocity and is given by 4.5 in Section 4.1. and is inserted into 4.13 and together with 4.4 forms the following system of differential equations:

$$c\frac{dQ}{dt} + g\left(\zeta_B - acos(\omega t)\right) = -\lambda_L Q \tag{4.14}$$

and

$$A_B \frac{\partial \zeta_B}{\partial t} = Q \tag{4.15}$$

where c is given as

$$c = \int_0^L \frac{1}{A} dx \tag{4.16}$$

As in Garrett & Cummins (2005), the integral in 4.16 is evaluated at the narrowest part of the channel with the cross sectional area A and length L. The constants are given in Table 4.1. and the differential equations are solved in matlab with the solver ode23 for non stiff differential equations. The decrease in average volume flux as λ_L increases is presented in Figure 4.6.

The power extracted from the current when the turbine friction is linear, is given as in 4.7 in Section 4.1. The result is given in Figure 4.7. As the time derivative term is of an order one ten times smaller than the pressure gradient, it is expected that the result obtained here will be very similar to the result in Section 4.1. The maximum power potential is estimated to be 89 MW and is achieved when the average volume flux is reduced to 16 490 m^3/s. The reduction from the estiamte given in Section 4.1 is larger than what expected and indicates that the time derivative might be of higher order, or the pressure gradient of lower. It should also be noted that the solution of the set of equation given in Figure 4.6 appears to be unstable for very small λ_L. This can be seen from the graph as it is not completely smooth and close to $\lambda_L = 0$ the solution makes a jump. But as the graph smoothens out for larger λ_L the solution is assumed to be correct and therefore the time derivative of greater importance than predicted.

Quadratic Friction

In Section 4.1 it is shown that the maximum power potential for quadratic friction is reduced to 98% of the maximum power potential for linear friction. Hence it is also assumed that introducing quadratic friction to 4.13, will reduce the estimated maximum power potential. The friction integrated over the length of the channel is given as 4.9 in 4.1. This gives the following system of differential equations:

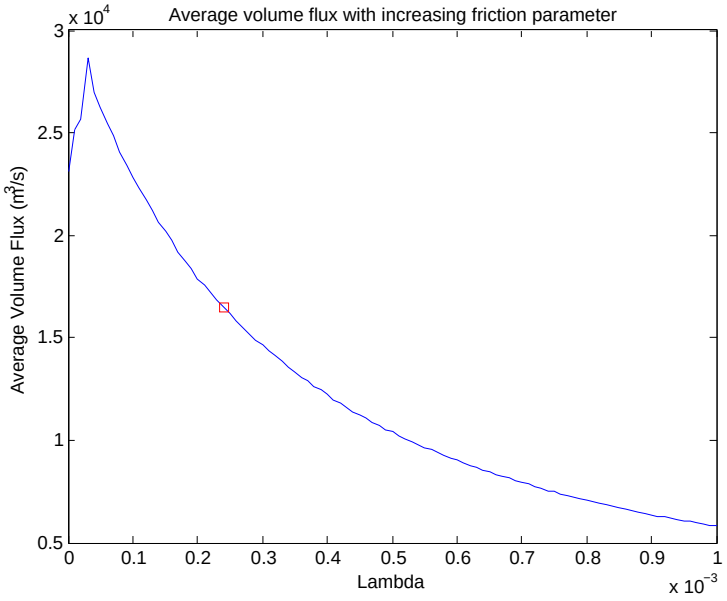

Figure 4.6: Average volume flux calculated from 4.14 and 4.15 with a balance between the time derivative of the volume flux, the pressure gradient and the resistance due to linear friction, for an increasing λ_L. The red square indicates the average volume flux when maximum power potential is reached, this is given in Figure 4.7

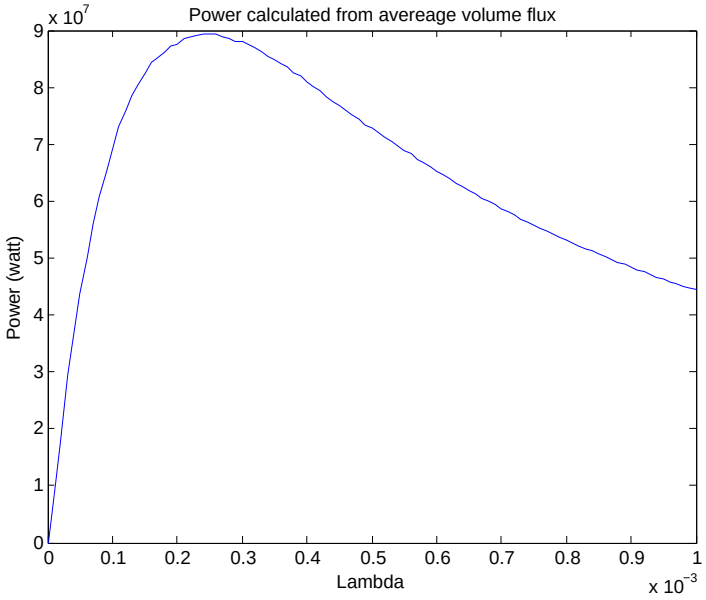

Figure 4.7: Power calculated from the 4.7 where the volume flux is calculated from 4.14 and 4.15 where the turbine friction is linear proportional to the velocity.

$$c\frac{dQ}{dt} + g\left(\zeta_B - acos(\omega t)\right) = -\lambda_S|Q|Q \tag{4.17}$$

and

$$A\frac{\partial \zeta_B}{\partial t} = Q \tag{4.18}$$

where c is given as in 4.16. The constants are given in Table 4.1, and the system of differential euqations is solved numerically in matlab with the same solver as for the linear case. The result is presented in Figure 4.8.

The power is calculated from 4.11 and from the results presented in Figure 4.9. The maximum power potential is 72 MW and is achieved when the average volume flux is reduced to 14 492 m^3/s, which is represented as a red square in Figure 4.8.

Similar to the solution of the linear case the the graph in Figure 4.8 is not smooth and indicates that the solution is not stable. The quadratic representation of the turbine friction reduces the power potential to 80 % of the

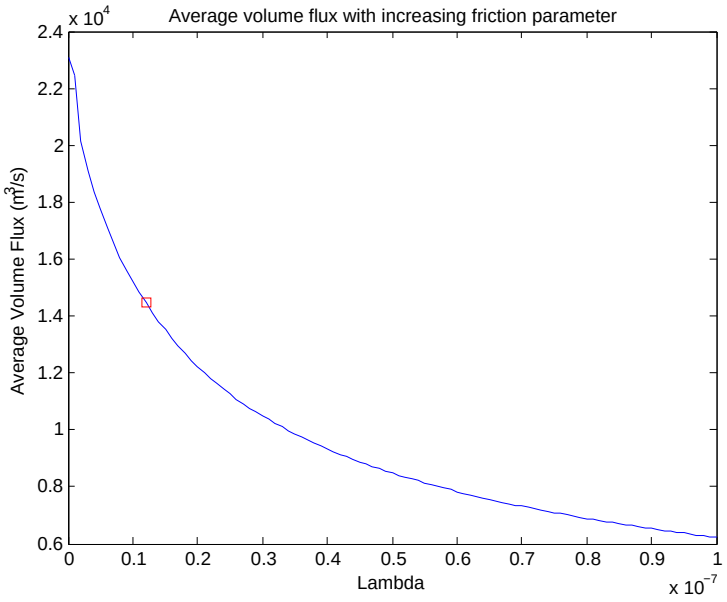

Figure 4.8: Average volume flux calculated from 4.17 and 4.18 with a balance between the time derivative of the volume flux, the pressure gradient and the resistance due to quadratic friction, for an increasing λ_S. The red square indicates the average volume flux when maximum power potential is reached. This is given in Figure 4.9

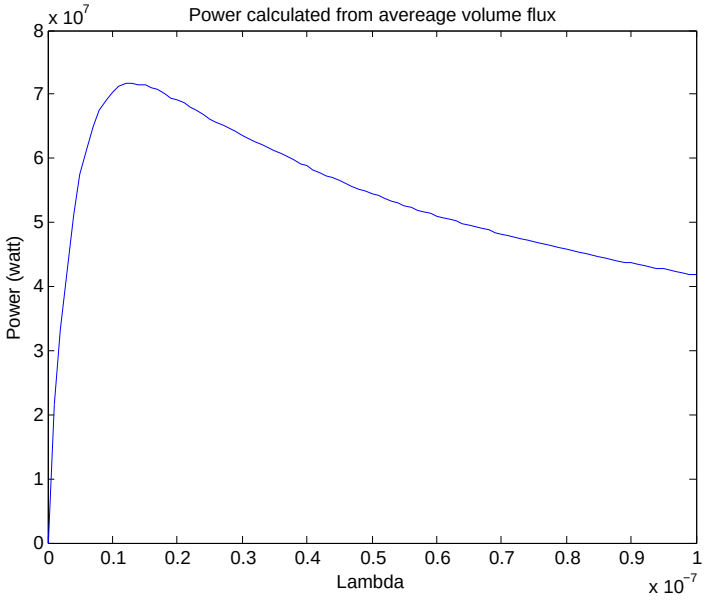

Figure 4.9: Power calculated from the 4.11. The volume flux is calculated from 4.17 and 4.18. The turbine friction is quadratic proportional to the velocity.

power potential given for the linear case.

4.3 Including the advection term

Integrating the entire 3.28 over the channel length gives the following equation:

$$\frac{dQ}{dt}\int_0^L \frac{1}{E}dx + +\frac{1}{2}\left(u^2(L) - u^2(0)\right) + g\left(\zeta_B - \zeta_0\right) = -\int_0^L \mathcal{F}_x dx \qquad (4.19)$$

where $x = 0$ is the channel entrance, $x = L$ is the channel exit, $u(0)$ is the velocity, and ζ_0 is the surface elevation at the channel entrance. $u(L)$ is the current velocity and ζ_B the surface elevation, both at the channel exit. The surface elevation at the entrance is given as $\zeta_0 = acos(\omega t)$, while ζ_B is affected by the energy extraction in the channel. The same assumptions are made as in Section 4.1 and Section 4.2, so the relationship between the

surface elevation in Balsfjord and the volume flux through Rystraumen is given by 4.4.

In the study done by Garrett &Cummins (2005) the velocity at the entrance is given as $u(0) = 0$. If the flow is drawn from an area with a large cross section, this is a reasonable assumption. Also for Rystraumen this is a reasonable assumption as already argued for in Section 3.2. The velocity at the exit is quite different, since here the flow is already accelerated and, as observed in Figure 3.1 in Section 3.2, continues as a jet into the pool on the east side of the channel. The same is also argued for in Garrett & Cummins (2005). If the current proceeds into the basin, there will be a loss of energy.

If the turbine friction is chosen to be represented by a quadratic relationship to the velocity, the integral of the friction term is given by:

$$\int_0^L \mathcal{F}_x dx = \lambda_S |Q|Q \tag{4.20}$$

An assumption which is already made, is that the volume flux through Rystraumen is only dependent of time and is given by $Q(t) = Au$. To find a representation of the velocity at the exit, the velocity $u^2(L)$ is expressed as:

$$\frac{1}{2}u^2(L) = \frac{1}{2}\frac{(A_e u)^2}{A_e^2} = \frac{1}{2}\frac{1}{A_e^2}|Q|Q \tag{4.21}$$

where the cross sectional area for Rystraumen is $A_e \approx 20000m^2$.

In this manner the effect of the energy loss due to the advection term can be included in the friction term:

$$c\frac{dQ}{dt} + g(\zeta_B - acos(\omega t)) = -\alpha|Q|Q \tag{4.22}$$

where

$$\alpha = \lambda + \frac{1}{2}\frac{1}{A_e^2} \tag{4.23}$$

The system of equations consisting of 4.22 and 4.4 has been solved in matlab with the ode23 solver for non stiff differentaial equations and presented in

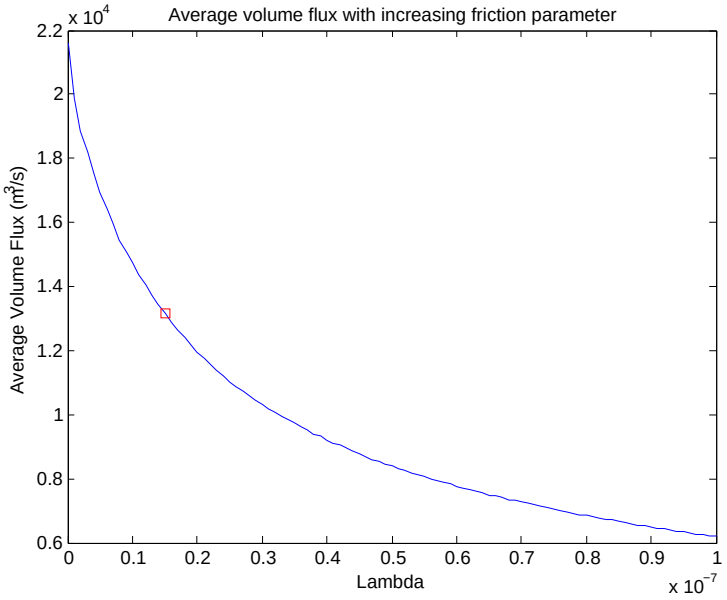

Figure 4.10: Average volume flux calculated from 4.22 and 4.4 with a balance between the time derivative of the volume flux, the advection term, the pressure gradient and the resistance due to quadratic friction, for an increasing λ_S. The red square indicates the average volume flux when maximum power potential is reached. This is given in Figure 4.11

Figure 4.10.

The power potential is calculated from 4.11 and the result is presented in Figure 4.11. The maximum power potential is 66 MW and is obtaines when the average volume flux is reduced to 13 155 m^3/s.

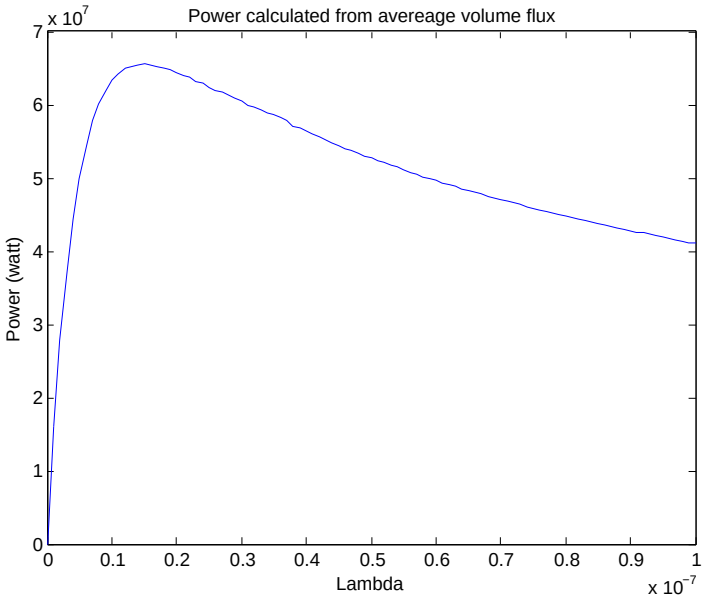

Figure 4.11: Power calculated from the 4.11. The volume flux is calculated from 4.22 and 4.4. The turbine friction is quadratic proportional to the velocity.

Chapter 5

Power potential from numerical simulations

5.1 FVCOM

To simulate the tide in the area around Rystraumen, the Finite-Volume Coastal Ocean circulation Model (called FVCOM) has been used. The model is fully described in the FVCOM User Manual [Chen et al., 2013] but the features important for the present work will be reviewed in this chapter. FVCOM has been developed specifically for the study of coastal oceanic and estuarine circulation and has been applied to several studies and compared successfully to measurements and results from other numerical models [Chen et al., 2003].

To simulate the tide along the coast of Troms a more cost-efficient version of FVCOM has been used; a two-dimensional vertical integrated model which has in previous studies proven to be successfully in describing the important features of tidal waters in coastal areas [Chen et al., 2011].

In the two-dimensional model, the effect of the temperature and salinity differences are not included, and the flow is incompressible. The two-dimensional model describing the flow is obtained by depth-integrating the governing equations given in Section 3.1: 3.1, 3.2, 3.3 and 3.4. The equations have been integrated over the water column $D = H + \zeta$ where H is the water depth and ζ is the surface elevation. The depth integrated equations are given as follows:

$$\frac{\partial \zeta}{\partial t} + \frac{\partial(\overline{u}D)}{\partial x} + \frac{\partial(\overline{v}D)}{\partial y} = 0 \tag{5.1}$$

$$\frac{\partial(\overline{u}D)}{\partial t} + \frac{(\partial \overline{uu}D)}{\partial x} + \frac{(\partial \overline{uv}D)}{\partial y} - fD\overline{v} - gD\frac{\partial \zeta}{\partial x} = -\frac{\tau_{bx}}{\rho_0} \tag{5.2}$$

$$\frac{\partial(\overline{v}D)}{\partial t} + \frac{(\partial \overline{uv}D)}{\partial x} + \frac{(\partial \overline{vv}D)}{\partial y} + fD\overline{u} - gD\frac{\partial \zeta}{\partial y} = -\frac{\tau_{by}}{\rho_0} \tag{5.3}$$

where the overbar indicates the average velocity over the depth, and τ_{bx} and τ_{by} are the x and y component of the bottom friction.

The equations have been discretized by the finite-volume method which is the most popular method in commercial computational fluid dynamics [Tu et al., 2008, Garg, 1998]. The advantege of the finite-volume method is that it combines the best from the finite-difference method and the finite-element method. It can handle both structured and unstructured grids and therefore can be applied to a large variation of geometries [Tu et al., 2008]. While the finite-difference and the finite-element methods solve the differential form of the equation, the finite-volume solves the equations on integral form. By discretization of the integral form of the governing equations, the basic quantities such as mass, momentum and energy will be conserved in each control volume. And if the numerical solutions are properly formulated, this method allows one to better comply to the conservations laws over the whole computational domain [Garg, 1998, Chen et al., 2013].

The computational domain has been divided into a set of non-overlapping unstructered triangular cells. Each cell consists of discrete points: three nodes, which make up the vertices of the triangle, and a centroid, which is placed in the middle of the triangle. The method makes use of the staggered grid approach where not all the function values have been defined in all the discrete points [Garg, 1998]. In the centroids of the cells the velocity components u and v are calculated. The scalar variables, the depth H and the surface elevation ζ, have been calculated in the nodes. The mean water depths at the nodes are given by the Norwegian Hydrographic Service.

The discretization method used is also the cell-vertex finite-volume method, meaning that the control volume is not always confined to one cell. While the momentum equation is calculated within one cell, the continuity equation is not. The latter has been calculated within an area enclosed by lines going

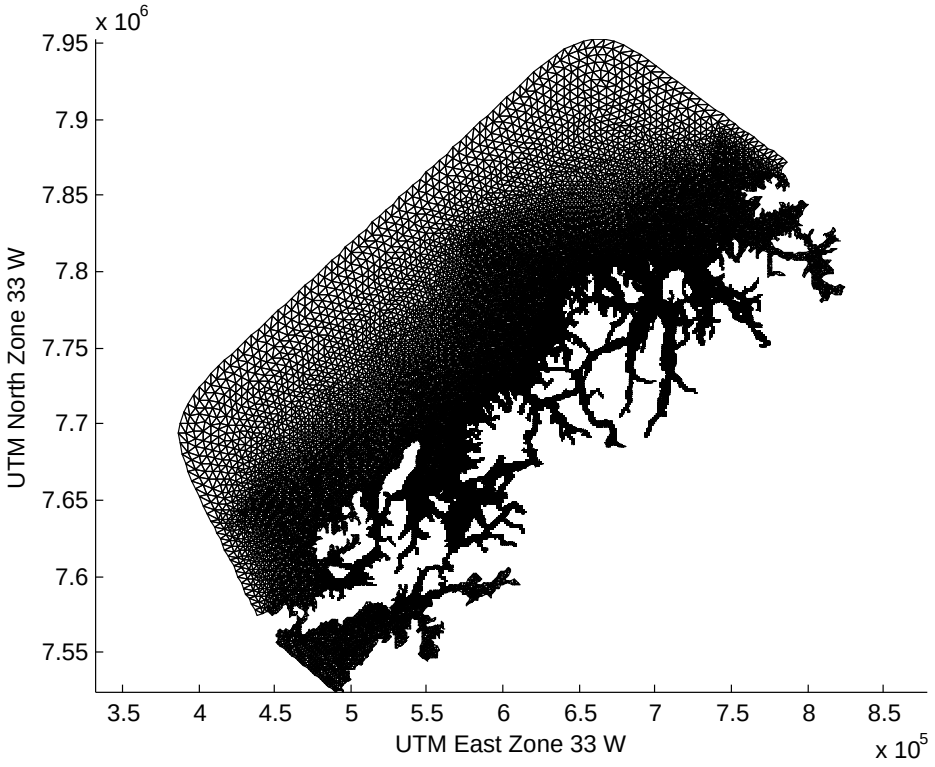

Figure 5.1: The computational domain for the model of Troms, from Vestrålen in the south to Sørøya in the north (FVCOM).

through the centroid and mid-points of the sides, surrounding one node. The governing equations are integrated over a given triangular area using a modified fourth-order Runge-Kutta time-stepping scheme, with second order accuracy [Chen et al., 2003].

The computational domain stretches from Vesterålen in the south to Sørøya in the north, as shown in Figure 5.1. The grid has a resolution varying from $5km$ at the outer boundaries to only $14m$ close to the coastline, when the shortest edge of the triangles is measured. In Rystraumen the resolution varies from 48-68m.

At the open boundaries in the west of the model domain the forcing is given as a sum of eight tidal constituents. The amplitude and the phase are given in Padman & Erofeeva (2004). As the velocities are calculated at the centroid of each cell there are no need to specify these at the boundary. The model is integrated over a time period of 100 days, where the equations are solved

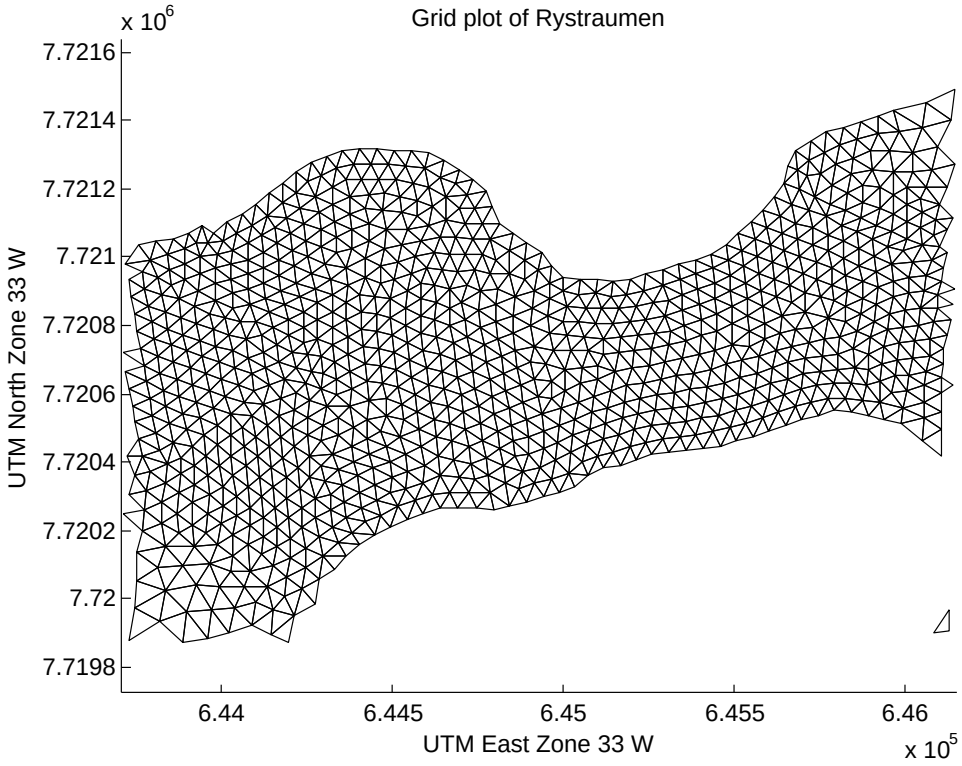

Figure 5.2: The grid over Rystraumen with a typical resolution of 50m (FVCOM)

at every 0.7 second and saved at every 15 minute. The bottom friction is calculated at each centroid from the equation:

$$\tau_{bx} = \rho C_D |\boldsymbol{V}| u \qquad (5.4) \qquad\qquad \tau_{by} = \rho C_D |\boldsymbol{V}| v \qquad (5.5)$$

where ρ is the density, $\boldsymbol{V}$ is the velocity and u and v are the x and y components of velocity, and C_D is the drag coefficient. The drag coefficient for bottom friction k_0 is for depths less than three meters given by $k_0 = 0.0027$ and for depths larger than three meters it is given as:

$$k_0 = g \left(\frac{H^\alpha}{NN} \right)^{-2} \qquad (5.6)$$

where g is the gravitational acceleration, H is the depth, $\alpha = 0.166667$ and $NN = 0.02$.

The model has not been validated against any measured values of current velocities or surface elevation, and there are therefore major unceratinties to the results obtained from the model simulations. The velocities obtained for Rystraumen from the model simulations are qualitatively compared to the results presented in Section 2.1. The maximum velocity given from simulations for the current in western direction is approximately $3.5 m/s$, as shown in Figure 5.3. This agrees well with what is reported in the study by Aquaterra Ltd, where the maximum velocity is $3.6 m/s$. Also for the current in eastern direction the velocities exceed $3 m/s$, as shown in the scatter plot in Figure 5.4.

5.2 Introducing turbines to the model

In the same way as in Sutherland et.al (2007) the turbine friction has been included in the bottom friction terms by adding extra drag in the cells where the turbines extract energy:

$$C_d = k_0 + k_t \qquad (5.7)$$

where k_0 is the friction coefficient associated with the natural bottom friction and k_t is the turbine friction [Sutherland et al., 2007].

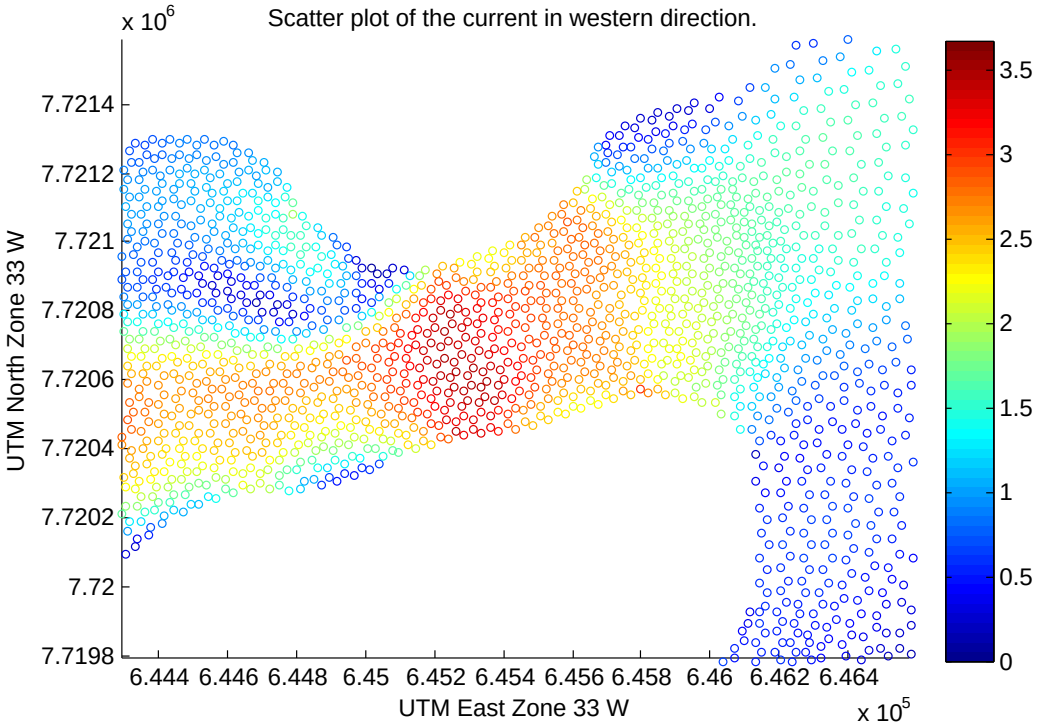

Figure 5.3: A scatter plot of Rystraumen of current in western direction. The maximum velocity is 3.5m/s

A uniform turbine fence covers the entire cross sectional area, as shown in Figure 5.5. The total energy dissipated in one grid cell both due to bottom friction and turbine friction, is calculated as in Sutherland et al. (2007):

$$P = \rho C_D |\overline{U^3}| A_{cell} \tag{5.8}$$

where ρ is the water density, $U = \sqrt{u^2 + v^2}$ is the velocity in the cell, and A_{cell} is the area of the cell. In these cell the drag coefficient is given by 5.7. The energy dissipation due to only turbines is calculated from the following equation:

$$P_t = \frac{k_t}{k_0 + k_t} P \tag{5.9}$$

The power extracted by the entire turbine fence across the channel is the sum of the power in each cell. The turbine friction is steadily increased, similar to what has been done in Sutherland et al. (2007). The result is presented in Figure 5.7.

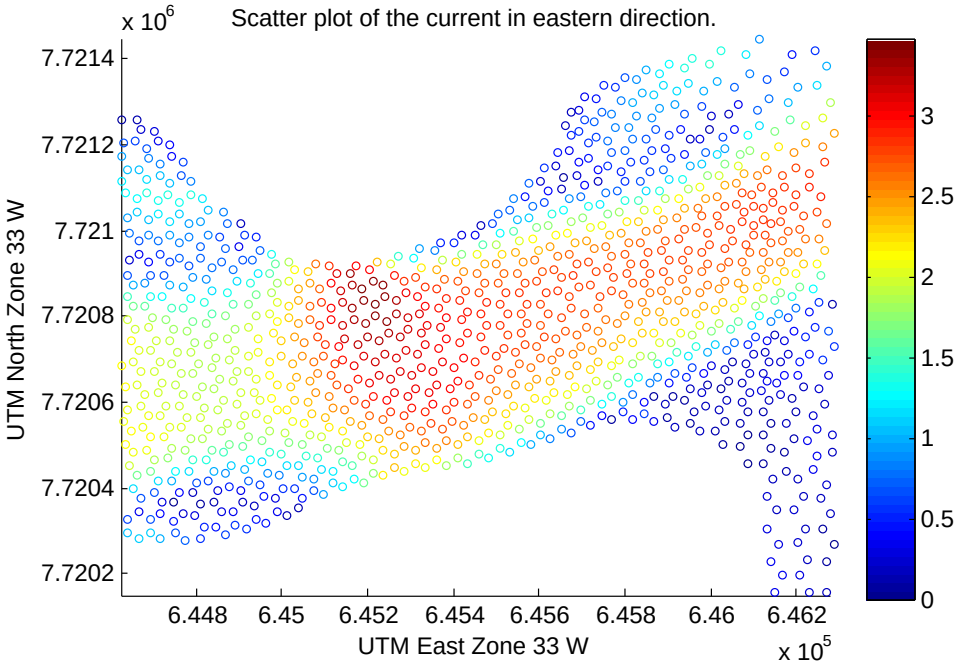

Figure 5.4: A scatter plot of Rystraumen of current in eastern direction. The maximum velocity is a bit less than 3.5m/s

What is seen in both the plot and the table is that the power increases fast until the power extraction reaches 38 MW. After 38 MW the energy dissipation due to turbine friction keeps increasing slowly. After 40 MW the graph flattens out. The turbine friction is increased up to 1.93 but when it is increased any further the model becomes unstable. For the highest turbine friction increases included the model only calculate for a few days before it is terminated for unknown reasons. However, based on how much the graph flattens out it is taken as a reliable estimate that the maximum power extraction is about 40 MW.

The volume flux is calculated through the cross section formed by adjacent nodes, where two and two nodes form the side of one triangle cell, as shown in Figure 5.6. Through each side the volume flux is calculated by multiplying the velocity normal to the side of the cell with the area spanned out by the same side and the depth. The velocity normal to the side found by a projection of the velocity vector down on this side. The total flux is given by summing up the volume flux through each cell. The volume flux is calculated for increasing turbine friction and the result is presented in Figure 5.8 and in Table 5.1. The maximum power potential of 40 MW is reached when the

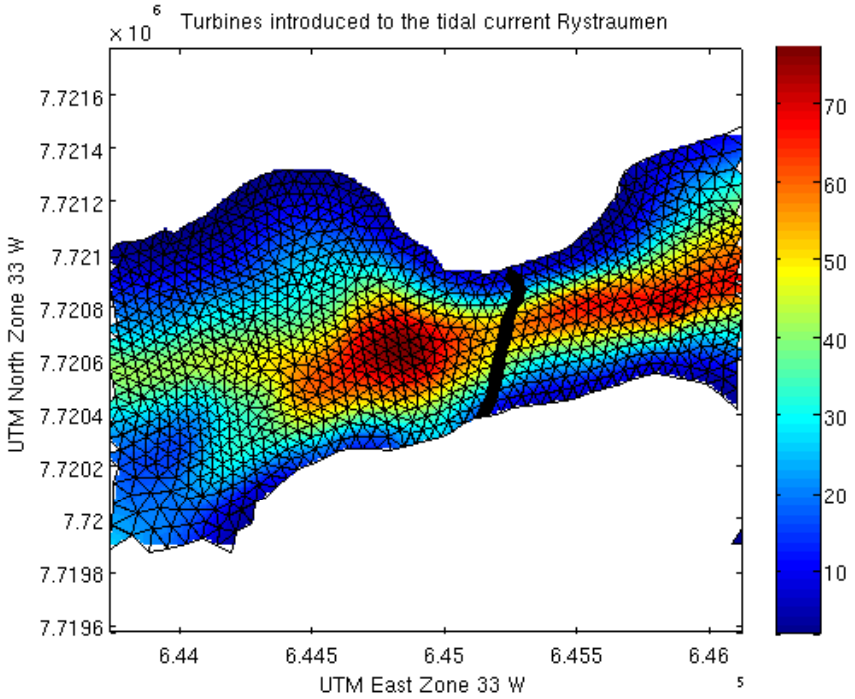

Figure 5.5: The turbine friction is added to the bottom friction in the pathced cells. The energy is extracted as a uniform turbine fence over the entire cross section of the channel.

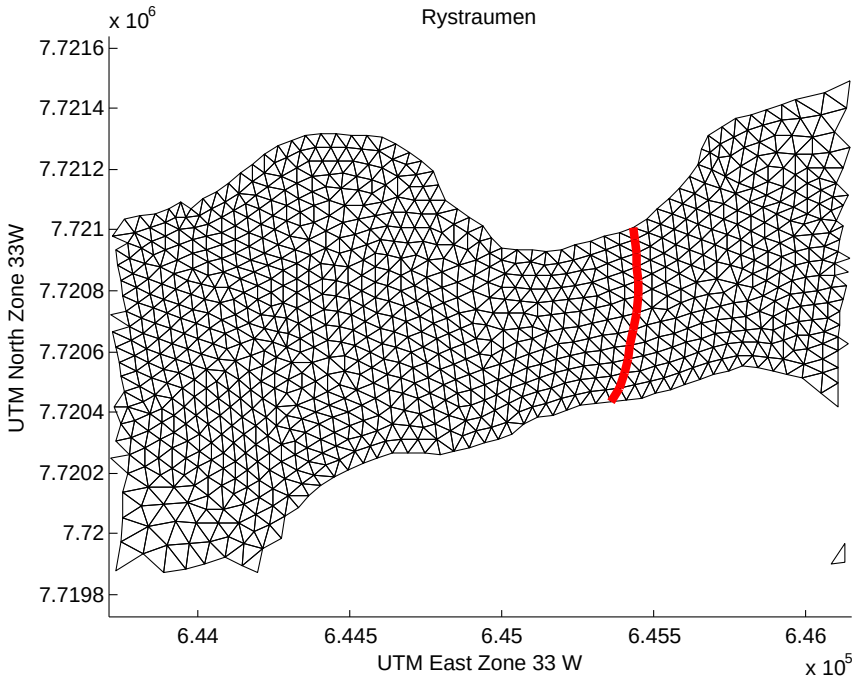

Figure 5.6: Adjacent nodes over a the width of the channel forms the cross sectional area which the volume flux through Rystraumen is calculated. (FVCOM)

average volume flux is reduced to 60% of the natural average volume flux.

5.3 Discussion

The estimate of the maximum power potential in Rystraumen calculated from the data obtained from the numerical simulations in FVCOM is expected to be more reliable than the theoretical estimate given in Chapter 4. The reason is that fewer simplifications are made in the governing equations given in Section 3.1. The difference between the estimate of 40 MW given in this chapter and the lowest estimate of 66 MW given in Chapter 4 will be discussed in this section.

In the esimates obtained in Chapter 4 the natural bottom friction is not included as it is unknown but assumed to be small. In the model the bottom friction is included, and if the assumption made in Chapter 4 is wrong, this might explain some of the difference in the estimates. For an average depth of $40m$ the bottom friction coefficient is calculated from 5.6 to be $k_0 = 0.001147$. The total energy dissipated over the entire bottom of the channel due to bottom friction is calculated from the following equation:

Turbine friction	Power MW	Peak volume flux	Average volume flux
0	0	58 164	28 029
0.10	12.404	51 895	26 258
0.20	20.271	48 099	24 870
0.30	25.711	46 033	23 827
0.40	29.377	42 978	22 919
0.50	31.936	40 754	22 111
0.60	33.620	39 059	21 343
0.70	35.036	38 355	20 705
0.80	36.030	37 165	20 138
0.90	37.017	35 939	19 640
1.00	37.737	35 318	19 208
1.10	38.257	34 676	18 796
1.15	38.452	33 852	18 635
1.20	38.666	34 070	18 483
1.25	38.819	32 977	18 307
1.30	39.003	33 423	18 117
1.35	39.093	32 393	17 932
1.40	39.325	32 043	17 786
1.45	39.380	31 679	17 639
1.50	39.519	31 870	17 477
1.55	39.675	31 275	17 335
1.60	39.847	30 707	17 185
1.65	39.849	30 559	17 052
1.70	40.093	30 527	16 929
1.75	40.139	30 183	16 797
1.80	40.243	29 850	16 669
1.85	40.535	29 393	16 565
1.90	40.380	29 483	16 433
1.92	40.677	29 393	16 386
1.93	40.601	29 081	16 367

Table 5.1: One fence is introduced to the current, while the friction is increased steadily to decide the maximum extractable power potential for the current.

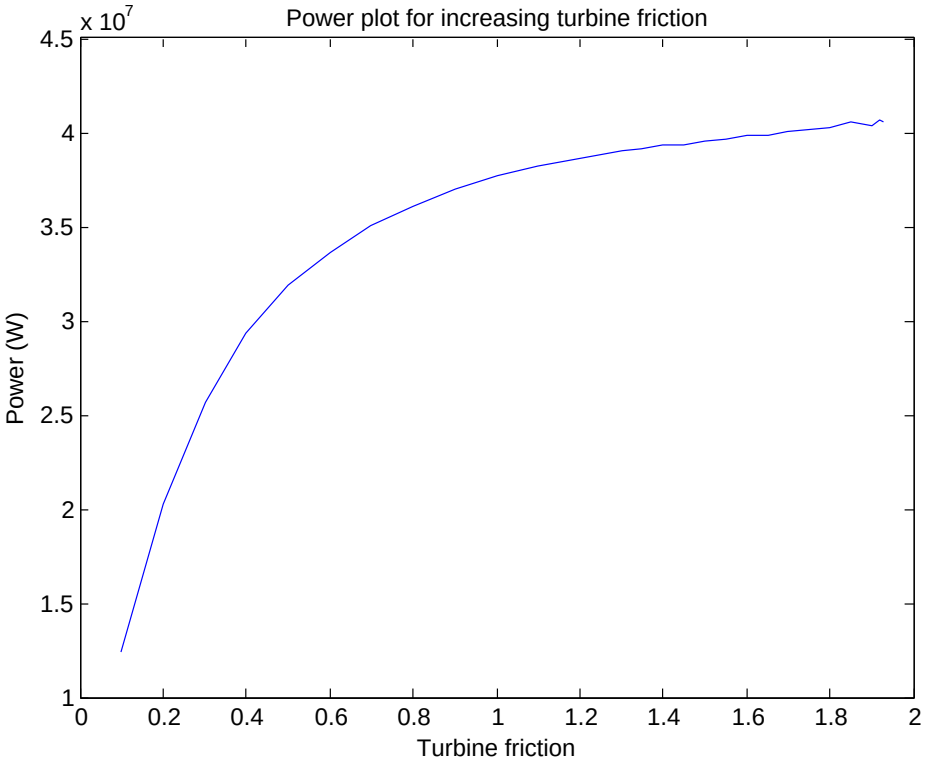

Figure 5.7: The power dissipated due to increased turbine friction in a uniform turbine fence across one entire cross section as shown in Figure 5.5.

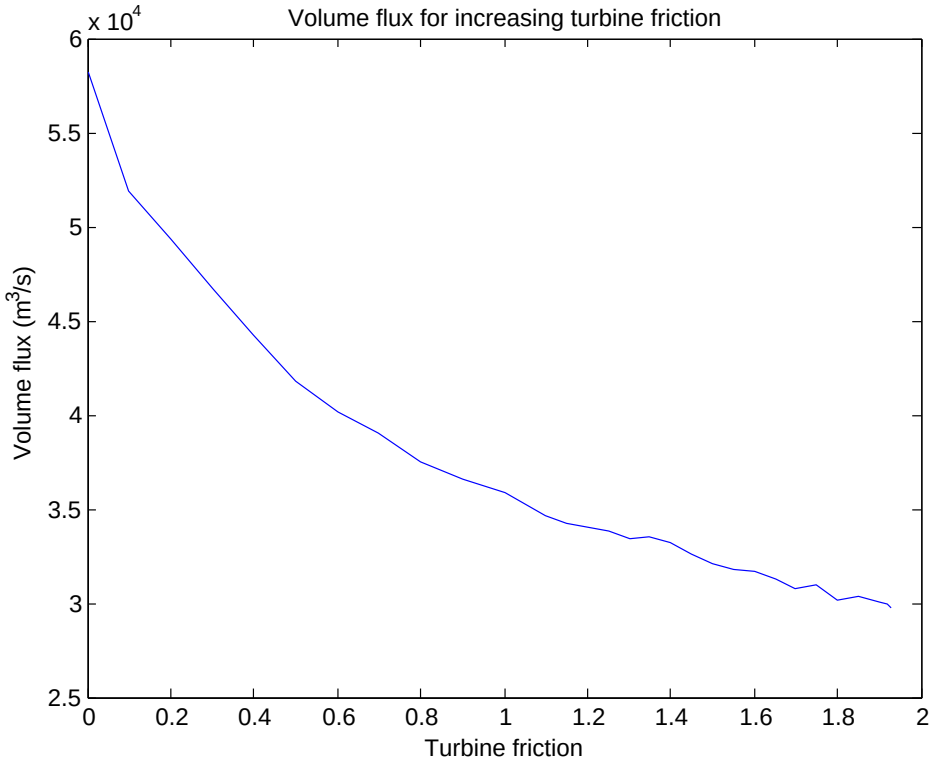

Figure 5.8: The decrease of peak volume flux through Rystraumen when the turbine friction is increased.

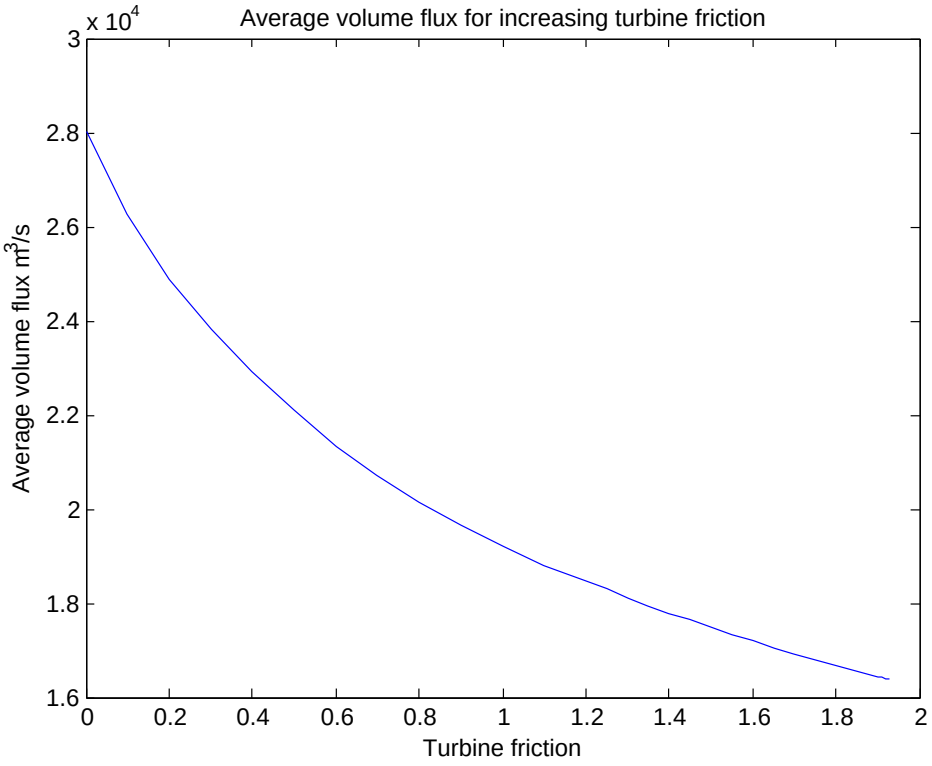

Figure 5.9: The decrease of average volume flux through Rystraumen as the turbine friction is increased.

$$P_0 = \rho k_0 |\overline{u}^3| A \tag{5.10}$$

where ρ is the density and given in Table 4.1, the average velocity is approximately $1m/s$ and the area of the channel is estimated to be $A = 10^6 m^2$. The total amount of energy dissipated over the channel bottom due to bottom friction is $P \approx 1$ MW. Based on this calculation it is very unlikely that the bottom friction can account for any large difference in the estimates. This confirms the assumption in Chapter 4 about the natural bottom friction being negligible.

The model describes the flow in Rystraumen by a two-dimensional model including the interaction with the flow of water through other narrow straits and fjords. In the theoretical estimates given in Chapter 4 it is assumed that the channels around Tromsø are closed, and that the water passing through Rystraumen flows into Balsfjord with Rystraumen as its only connection to the rest of the sea. Clearly this is not the case, but it is a reasonable simplification, as the velocity of the currents on both sides of Tromsø is less than $1m/s$ as shown in Figure 5.10. But, when the theoretical estimate is calculated to be 26 MW higher than the estimate calculated from the numerical simulations, it is natural to assume that the simplification identical to viewing Balsfjord as a closed bay is the main reason for the large difference.

As the flow through Rystraumen meets a higher resistance due to turbine friction, the flow of water might be diverted away from the channel. For the flow in western direction, a higher resistance in Rystraumen might divert the flow into Balsfjord instead. Another possibility is that when the flow meets a higher resistance in Rystraumen, the flow of water is diverted to the channel parallel with Rystraumen but on the other side of Rysøya. The direction which the flow is diverted in is dependent on the relative resistance between the channel from which the energy is extracted and the channel which the flow can be diverted into [Atwater and Lawrence, 2010]. As the channel south of Ryøya is very shallow, the resistance is expected to be very high, and therefore it is unlikely that large masses of water will be diverted into this channel. How the energy extraction will affect the volume flux into Balsfjord is not investigated in this study, and some of the difference between the theoretical and modelled estimate can be explained by an increased volume flux into this channel. In Sutherland et al. (2007) two cases were studied in which the flow could be diverted away from the channel with turbines in it. In these two cases the modelled dissipation was 46% to 69% of the theroetical estimate.

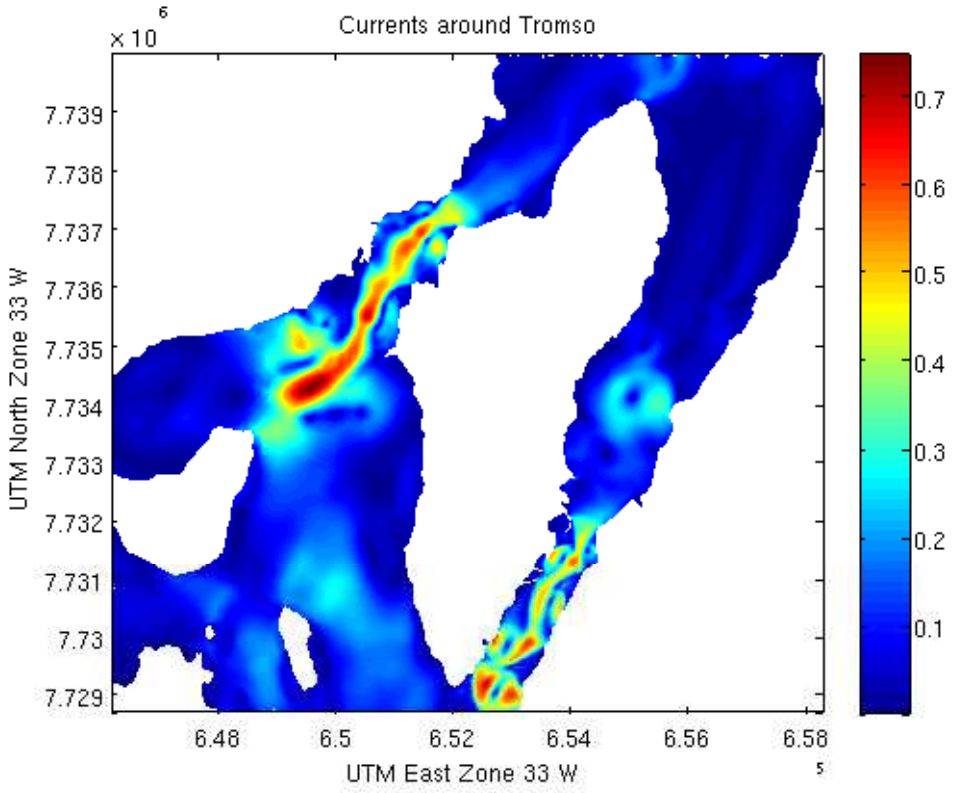

Figure 5.10: A plot of the current around the island Tromsø where the maximum current velocity is approximately $0.7m/s$

Also the maximum power potential obtained from the numerical simulations are overestimated. The energy is dissipated over a whole cross section of the channel. There are several reasons why this is not possible. Turbines have to be placed at locations where the sea floor has low gradients. From Figure 2.2 it can be seen that this is true only for the middle parts of the channel, and therefore turbines cannot be placed over the entire cross section. Placing turbines over only a fraction of the channel width will lower the power potential [Garrett and Cummins, 2008]. The turbines also require a certain depth in the channel and the Flumill turbines will be 30 meters tall. The turbines can not be in conflict with ships going through the channel and can therefore not cover the entire cross section close to the surface.

It is also important to emphasize that 40 MW is the maximum energy that can be dissipated due to turbines in the current and not the power produced by the turbine. Drag on the supporting structure of the installation is included in the dissipate energy due to turbine friction [Garrett and Cummins, 2008] . This cannot be converted to electrical energy. Also when energy is converted to electrical energy, there will be a loss. The estimate of 40 MW is therefore a maximum estimate of the power which can be extracted from the tidal current in Rystraumen.

Chapter 6

Conclusion

The tidal energy extraction device, Flumill 0.5 MW, is ready for being tested in natural environments in Rystraumen close to Tromsø. If the testing goes well, three larger tidal devices will be extracting up to 5 MW from the current within few years. In this respect it is wanted to decide the maximum power avalable for extraction from the current in Rystraumen. This is done in this study both by theroetically and by use of a numerical model (FVCOM).

In the theoretical study the flow in Rystraumen is described by a single governing equation consisting of an acceleration term, a pressure gradient term and the force associated with turbine friction. The importance of the different terms is investigated and it is concluded that they are all important for the estimation of the power potential for the case studied here. When only the pressure gradient, the driving force of the flow, is included, the maximum power potential is estimated to be 93 MW when the turbine friction is given as proportional to the velocity squared. With the same turbine friction representation, the estimated maximum power potential is lowered to 66 MW when all terms are included.

Still, the lowest estimate given from the theoretical study is higher than the estimate obtained from the numerical model and more consideration is needed in order to give a more accurat estimate of the maximum power potential of Rystraumen. The main reason for the high estimate is assumed to be the simplification done with respect to the channels on each side of Tromsø. The volume flux through these channels are neglected and instead Balsfjord is viewed as a closed bay, with Rystraumen as its only connection to the sea outside. The high estimate indicates that also the currents neglected

in this study must be included to give a better estimate of the maximum power potential. Also the bottom friction is neglected in the study as well as the possibility for the flow to be diverted away from the channel. However, these simplifications are expected to be of less importance.

With the depth integrated two-dimensional version of FVCOM the flow through Rystraumen is simulated, and from the velocity data obtained from the simulations the maximum power potential is estimated. The estimate given here is expected to be more accurate, as fewer simplifications are made. The turbines are included in the model by adding an additional friction coefficient in cells forming a fence across the narrowest part of the channel. The friction coefficient associated with turbine friction is steadily increased until the maximum power potential of 40 MW is obtained. After this peak is reached, the power dissipated does not change when the turbine friction coefficient is further increased.

It is important to emphasize that this is the maximum energy which can be dissipated, not extracted. Drag from supporting structure of the tidal power devices is not taken into account in this study and neither are efficiency factors for converting the kinetic energy into electrical energy. The estimate is also obtained under the assumption that the entire cross section is available for extraction, but since boats pass through, this is not realistic. However, this is a valuable estimate of the maximum power available for extraction in Rystraumen.

6.1 Future work

There are three main areas in which further work can be recommended: further work with the theoretical estimate, further work with the estimate from the numerical model, and studies of the environmental impact of the energy extraction.

In the theoretical study the volume flux through the channels on both sides of Tromsø should be included as it will probably contribute to a more accurate estimate of the maximum power potential in Rystraumen.

As it is more realistic to only extract energy from parts of the channel, further work should include a study where one or several partial fences only cover a fraction of the channel. This can be done both in a theretical study and by numerical simulations. From model simulations also the optimum location

for turbines can be decided both from a two-dimensional model and even more accurate with a three-dimensional numerical model.

When the model is validated for the whole computational domain, the study can quite easily be extended to a study of the environmental impacts of energy extraction in and around Rystraumen. A further study should include any change in volume flux in nearby fjords and straits, and whether any change in surface elevation occurs as a result of energy extraction in Rystraumen. A more extensive suggestion to further work would be to include sediment transport into the model in order to decide whether or not energy extraction will have an impact on sedimentation processes both locally and far afield.

References

[Aquatera Ltd, 2013] Aquatera Ltd (2013). Vessel Mounted ADCP survey typical report. Technical report, Aquatera Ltd, Stromsness.

[Atwater and Lawrence, 2010] Atwater, J. F. and Lawrence, G. A. (2010). Power potential of a split tidal channel. *Renewable Energy*, 35(2):329–332.

[Bryden et al., 2004] Bryden, I., Grinsted, T., and Melville, G. (2004). Assessing the potential of a simple tidal channel to deliver useful energy. *Applied Ocean Research*, 26(5):198–204.

[Carballo et al., 2009] Carballo, R., Iglesias, G., and Castro, a. (2009). Numerical model evaluation of tidal stream energy resources in the Ría de Muros (NW Spain). *Renewable Energy*, 34(6):1517–1524.

[Charlier, 2003] Charlier, R. H. (2003). A sleeper awakes: tidal current power. *Renewable and Sustainable Energy Reviews*, 7(6):515–529.

[Chen et al., 2013] Chen, C., Beardsley, R. C., Cowles, G., Qi, J., Lai, Z., Gao, G., Stuebe, D., Liu, H., Xu, Q., Xue, P., Ge, J., Hu, S., Ji, R., Tian, R., Huang, H., Wu, L., Lin, H., Sun, Y., and Zhao, L. (2013). An Unstructured Grid , Finite-Volume Community Ocean Model FVCOM User Manual.

[Chen et al., 2011] Chen, C., Huang, H., Beardsley, R. C., Xu, Q., Limeburner, R., Cowles, G. W., Sun, Y., Qi, J., and Lin, H. (2011). Tidal dynamics in the Gulf of Maine and New England Shelf: An application of FVCOM. *Journal of Geophysical Research*, 116.

[Chen et al., 2003] Chen, C., Liu, H., and Beardsley, R. C. (2003). An Unstructured Grid, Finite-Volume, Three-Dimensional, Primitive Equations Ocean Model: Application to Coastal Ocean and Estuaries. *Journal of Atmospheric and Oceanic Technology*, 20:159–186.

[Defne et al., 2011] Defne, Z., Haas, K. a., and Fritz, H. M. (2011). Numerical modeling of tidal currents and the effects of power extraction on estuarine hydrodynamics along the Georgia coast, USA. *Renewable Energy*, 36(12):3461–3471.

[Draper et al., 2014] Draper, S., Adcock, T. A., Borthwick, A. G., and Houlsby, G. T. (2014). Estimate of the tidal stream power resource of the Pentland Firth. *Renewable Energy*, 63:650–657.

[Elliot, 2004] Elliot, D. (2004). Tidal Power. In *Renewable Energy*, pages 148–192. Oxford University Press, Oxford, 2nd. edition.

[Enova, 2014] Enova (2014). Flumill: Kjempeskruer skal gjore tidevann elektrisk. `http://www.enova.no/finansiering/naring/aktuelt/flumill-kjempeskruer-skal-gjore-tidevann-elektrisk/250/948/`. Accessed: 2014-03-09.

[Enova SF, 2007] Enova SF (2007). Potensialstudie av havenergi i Norge.

[European Commission, 1996] European Commission, R. (1996). Non nuclear energy JOULE II Wave energy Project results The exploitation of tidal marine currents. Technical report, Directorate_General Science, Research and Development.

[Flumill, 2011] Flumill (2011). Konsesjonssøknad utplassering av Tidevannsanlegg Rystraumen.

[Flumill, 2014] Flumill (2014). Flumill. `http://www.flumill.com`. Accessed: 2014-03-09.

[Garg, 1998] Garg, V. e. (1998). *Applied Computational Fluid Dynamics*. Marcel Dekker Inc, Colombus,Ohio, 1st edition.

[Garrett and Cummins, 2004] Garrett, C. and Cummins, P. (2004). Generating Power from Tidal Currents. *Journal of Waterway,Port,Coastal and Ocean Engineering*, 130:114–118.

[Garrett and Cummins, 2005] Garrett, C. and Cummins, P. (2005). The power potential of tidal currents in channels. *Proceedings of the Royal Society A: Mathematical, Physical and Engineering Sciences*, 461(2060):2563–2572.

[Garrett and Cummins, 2008] Garrett, C. and Cummins, P. (2008). Limits to tidal current power. *Renewable Energy*, 33(11):2485–2490.

[GeoNord Survey Team, 2013] GeoNord Survey Team (2013). Rystraumen in TromsøSidescan survey report. Technical Report 12152, GeoNord Survey Team.

[Google, 2014] Google (2014). Google Maps. `https://maps.google.com/`. Accessed: 2014-03-14.

[Grabbe et al., 2009] Grabbe, M. r., Lalander, E., Lundin, S., and Leijon, M. (2009). A review of the tidal current energy resource in Norway. *Renewable and Sustainable Energy Reviews*, 13(8):1898–1909.

[Marshall and Plumb, 2008] Marshall, J. and Plumb, A. R. (2008). *ATMOSPHERE, OCEAN AND CLIMATE DYNAMICS: AN INTRODUCTORY TEXT*. Elsevier Inc., Massachusetts, 1 edition.

[Padman and Erofeeva, 2004] Padman, L. and Erofeeva, S. (2004). A barotropic inverse tidal model for the Arctic Ocean. *Geophysical Research Letters*, 31(2).

[Plew and Stevens, 2013] Plew, D. R. and Stevens, C. L. (2013). Numerical modelling of the effect of turbines on currents in a tidal channel Tory Channel, New Zealand. *Renewable Energy*, 57:269–282.

[Pugh, 1987] Pugh, D. (1987). *Tides, Surges and Mean Sea-Level*. John Wiley and Sons Ltd., Swindon,UK, 1 edition.

[Rourke et al., 2010] Rourke, F. O., Boyle, F., and Reynolds, A. (2010). Tidal energy update 2009. *Applied Energy*, 87(2):398–409.

[Sutherland et al., 2007] Sutherland, G., Foreman, M., and Garrett, C. (2007). Tidal current energy assessment for Johnstone Strait, Vancouver Island. *Proceedings of the Institution of Mechanical Engineers, Part A: Journal of Power and Energy*, 221(2):147–157.

[Tu et al., 2008] Tu, J., Yeoh, G. Y., and Liu, C. (2008). *Computational Fluid Dynamics, A Practical Approach*. Elsevier Inc., Burlington, 1st edition.

[Vennell, 2011] Vennell, R. (2011). Estimating the power potential of tidal currents and the impact of power extraction on flow speeds. *Renewable Energy*, 36(12):3558–3565.

[White, 2011] White, F. M. (2011). *Fluid Mechanics*. McGraw-Hill Companies, Inc., New York, 7 edition.